




## Research Article

# Prediction Model of Rate Decline for Acid-Fracturing Vertical Wells in Pore-Cavity-Fracture Carbonate Reservoirs

Mingxian Wang <sup>1</sup>, Zifei Fan,<sup>2</sup> Zhifeng Zhu,<sup>3</sup> Qingli Wang,<sup>3</sup> Lun Zhao <sup>2</sup>, Wenqi Zhao <sup>2</sup>, and Chengqian Tan<sup>1</sup>

<sup>1</sup>School of Earth Science and Engineering, Xi'an Shiyou University, Xi'an 710065, China

<sup>2</sup>Research Institute of Petroleum Exploration and Development, PetroChina, Beijing 100083, China

<sup>3</sup>No. 4 Oil Production Plant of Changqing Oilfield Company, PetroChina, Xi'an 710021, China

Correspondence should be addressed to Mingxian Wang; wangmingxian@xsyu.edu.cn

Received 26 May 2022; Accepted 14 July 2022; Published 17 August 2022

Academic Editor: Wenhui Li

Copyright © 2022 Mingxian Wang et al. This is an open access article distributed under the Creative Commons Attribution License, which permits unrestricted use, distribution, and reproduction in any medium, provided the original work is properly cited.

In view of the lack of rate decline prediction model of acid-fracturing vertical wells (AFVWs) in pore-cavity-fracture carbonate reservoirs, a prediction model of AFVWs with consideration of wormholes and fractures generated by acid fracturing is established by using the idea of compound reservoir. Acid fracturing significantly increases well productivity in the early period, but in the late period, its impact on instantaneous and cumulative production almost disappears. A higher interzonal diffusivity ratio or a lower interzonal conductivity ratio generated by acid fracturing can bring a better stimulation effect in the early period. Three typical production stages can be observed on the conventional productivity curves under constant wellbore pressure, corresponding to early linear decline stage, middle stable production stage, and late depletion decline stage, respectively. A new productivity function is defined by using a pseudo-steady state constant, and a set of new type rate decline curves of AFVWs in pore-cavity-fracture carbonate reservoirs is plotted and presented. Six typical flow regimes can be identified on these new type curves, including two or three V-shaped segments. The duration of all flow regimes and the depth and amplitude of V-shaped segments are controlled by interzonal diffusivity ratio, interzonal conductivity ratio, elastic storability ratio, crossflow coefficient, and boundary conditions. Reservoir parameter interpretation and future productivity prediction for an oil well in North Truva Oilfield were conducted by using our proposed model. The prediction results are consistent with the actual production, proving our model's accuracy and reliability. Compared with the conventional rate decline curves, these new type rate decline curves have more prominent flow regimes and can improve well-test inversion accuracy, reduce shut-in time, and increase well productivity.

## 1. Introduction

Carbonate reservoirs always develop a variety of pore structure composite types, and pore-cavity-fracture reservoir is one of the most important composite types [1]. This reservoir type is widely distributed in major carbonate oilfields around the world, such as Rumaila oilfield in Iraq, North Truva oilfield in Kazakhstan, and Tarim oilfield in China [2–4]. Fluid flow in pore-cavity-fracture carbonate reservoir can be characterized by a triple-continuum flow system. Liu et al. first proposed a mathematical model to describe the seepage behavior in a triple media system on the basis of

classical Warren-Root dual-media model [5, 6]. Furthermore, Wu et al. studied the single-phase flow and multi-phase flow in pore-cavity-fracture carbonate reservoir based on Liu et al.'s model and analyzed its seepage behavior and parameter sensitivity [7, 8]. Acid fracturing is an effective stimulation technology for carbonate reservoirs, which works by forming fractures and wormholes with high conductivity through hydraulic action and acid dissolution (Figures 1 and 2) and improving reservoir seepage capacity near bottomhole [9]. At present, the research on acid fracturing focuses on acid fluid system and construction technology [10–12], but a proper prediction model for rate

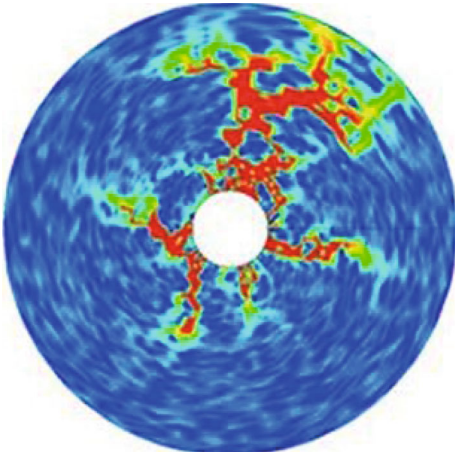


FIGURE 1: Wormholes generated by acid fluid dissolution [6].

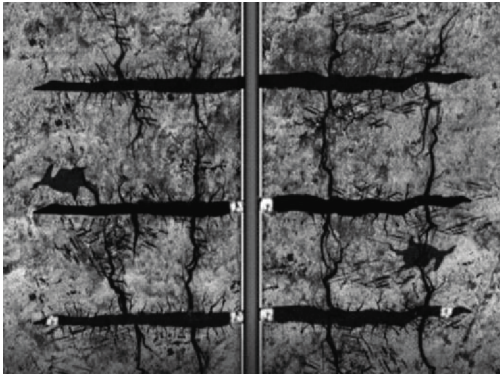


FIGURE 2: Fractures and wormholes in vertical wells generated by acid fracturing.

decline of acid-fracturing vertical wells (AFVWs) is still lacking in pore-cavity-fracture carbonate reservoirs, which brings difficulties and challenges to productivity estimation and well-test interpretation of these stimulation wells.

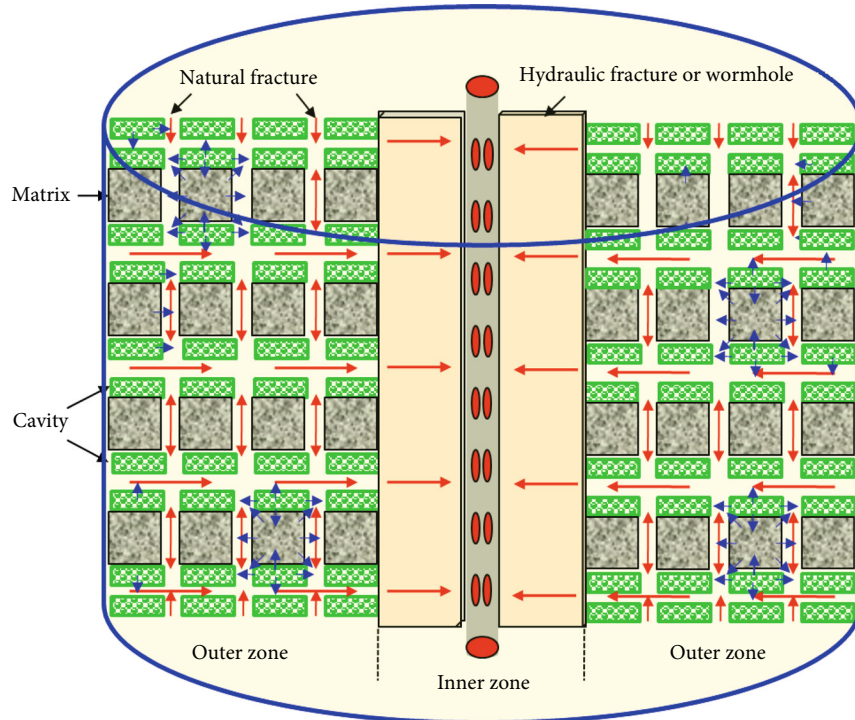
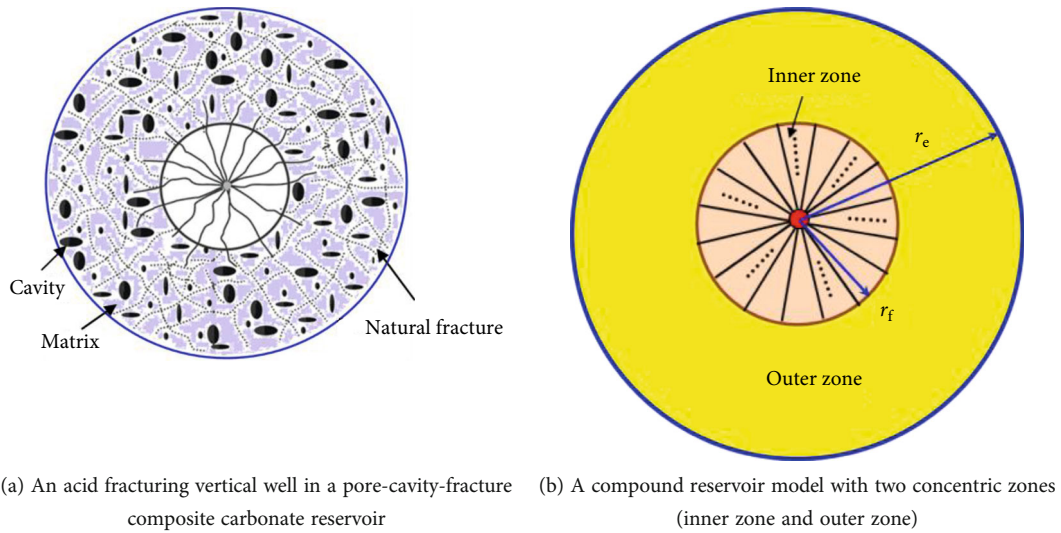
The key point of establishing a suitable prediction model of rate decline for AFVWs is to take fractures and wormholes into account. However, a comprehensive consideration of highly heterogeneous proppant placement in a fracture and complex profile of fracture wall eroding by injected acids is not easy when establishing a productivity model. In nature, wormholes can be simplified and conceptualized as fractures with large width. Under this circumstance, the flow in these wormholes can be treated with the seepage theory of hydraulic fractures, and the flow in an acid-fracturing well transforms into the problem of multiple fractures. Fortunately, the evaluation of fractured well productivity has been a well-developed engineering science [13]. Many classic models of fractured well productivity have been developed by considering planar vertical fractures with simple rectangular geometry and uniform conductivity [14–16] and lay a solid foundation for later comprehensive evaluation of fractured well production. In the past two decades, hydraulic fracturing and acid fracturing achieved great success in the effective development of unconventional reservoirs and attracted an increasing attention on fractured well produc-

tivity. More realistic fracture shapes, nonuniform conductivity distributions, and complex fracture properties were coupled in fractured well modeling [17–20], which provides an idea for the establishment and solution of a rate decline model for AFVWs. At the same time, there has been a lot of research on the problem of multiple fractures. Restrepo used the idea of compound reservoir to deal with multiple fractures formed by hydraulic fracturing, but a redundant minus sign in the boundary condition resulted in the mask of many seepage characteristics [21]. Wang et al. used the point source function integral idea to establish a mathematical model considering wormhole in a compound carbonate reservoir and focused on the transient pressure analysis [22]. Chen et al. proposed an approximate analytical productivity equation for fractured wells with multiple asymmetrical fractures in low-permeability and anisotropic cylinder-shaped formations using conformal mapping and mirror reflection [23]. Chuprakov et al. developed a numerical model of hydraulic fracture productivity considering heterogeneous distribution of conductivity and channels and presented its application in productivity assessments [24]. In general, there are many researches on the rate decline of fractured wells, but the study of multifracture problem like acid fracturing mainly focuses on unstable seepage behavior and steady-state productivity. The existing relevant models cannot meet the requirements of rapid well-test inversion and actual productivity prediction, especially for acid-fracturing vertical wells in the pore-cavity-fracture composite carbonate reservoirs.

In this study, the idea of compound reservoir and grid discretization is used to establish a rate decline prediction model of acid-fracturing vertical wells with consideration of acid-eroded fractures and wormholes in the pore-cavity-fracture carbonate reservoirs. Both conventional and new type rate decline curves are plotted and presented to analyze the rate decline behavior and production sensitivity of AFVWs, and a field example is selected for the application and verification of the proposed model. These new type rate decline curves can improve the accuracy of well-test interpretation and reduce shut-in time, and finally increase well productivity.

## 2. Compound Flow Model of an AFVW in a Pore-Cavity-Fracture Carbonate Reservoir

**2.1. Physical Model and Model Assumptions.** Pore-cavity-fracture composite carbonate reservoir is a typical triple media reservoir from the relevant literature [5–8]. After acid fracturing operation, a complex fracture network system (acid-eroded fractures and wormholes) is generated in the formation near wellbore, creating an artificial high permeability area (Figure 3(a)). Combined with the characteristics of fracture network system in an acid-fracturing well (Figures 1 and 2), the stimulated area can be equivalent to a multiple artificial fracture or wormhole system with infinite conductivity and approximate equal length (Figure 3(b)). Under this condition, acid-fracturing vertical wells can be regarded as a compound reservoir model. This compound model consists of two concentric zones, namely, inner zone (acid fracturing



(c) A sectional view of fluid transport in the compound model

FIGURE 3: Schematic diagram of a compound flow model of acid fracturing vertical well in a pore-cavity-fracture carbonate reservoir.

stimulated area) and outer zone (pore-cavity-fracture composite formation) (Figures 3(b) and 3(c)).

In the outer zone, natural fractures are the main flow channel and directly connect with multiple artificial fracture or wormhole system in the inner zone. Crude oil in the matrix system first flows into natural fractures and then into the vertical wellbore through the fracture network system in the inner zone; crude oil in the cavity system can directly flow into natural fractures and also can flow into matrix pores first and then into natural fractures. In the inner zone, only acid-eroded fractures and wormholes directly connect to the wellbore and provide the fluid seepage channel (Figure 3). In order to build up a rate decline prediction model of AFVWs in pore-cavity-fracture carbonate reser-

voirs, the basic assumptions of the model are made as follows:

- (1) In the inner zone,  $N$  acid-eroded fractures and wormholes are formed after acid fracturing. All acid-eroded fractures and wormholes have the same width and permeability and vertically penetrate throughout the whole formation, through which fluid flows into vertical wellbore. The radius of the inner zone is equal to the half-length of acid-eroded fractures or wormholes
- (2) The reserves of pore-cavity-fracture carbonate reservoirs can be dominated by matrix system or cavity

TABLE 1: Definitions of dimensionless variables.

Dimensionless parameters	Definitions
Pressure in inner zone	$p_{1D} = k_{2f}h(p_i - p_1)/1.842q\mu B$
Pressure of natural fracture system in outer zone	$p_{2fD} = k_{2f}h(p_i - p_{2f})/1.842q\mu B$
Production time	$t_D = 3.6k_{2f}t/\mu(\phi_{c_t})_{2f}r_f^2$
Radial distance	$r_D = r/r_f$
Reservoir radius	$r_{eD} = r_e/r_f$
Wellbore radius	$r_{wD} = r_w/r_f$
Interzonal diffusivity ratio	$\alpha = \eta_{2f}/\eta_1 = k_{2f}(\phi_{c_t})_1/k_1(\phi_{c_t})_{2f}$
Interzonal conductivity ratio	$\beta = 2\pi k_{2f}r_f/nbk_1$
Matrix-fracture crossflow coefficient	$\lambda_{mf} = \gamma_{mf}k_{2m}r_f^2/k_{2f}$
Cavity-fracture crossflow coefficient	$\lambda_{cf} = \gamma_{cf}k_{2c}r_f^2/k_{2f}$
Cavity-matrix crossflow coefficient	$\lambda_{cm} = \gamma_{cm}k_{2c}r_f^2/k_{2f}$
Elastic storability ratio of natural fracture system	$\omega_{2f} = (\phi_{c_t})_{2f}/(\phi_{c_t})_{2f} + (\phi_{c_t})_{2m} + (\phi_{c_t})_{2c}$
Elastic storability ratio of matrix system	$\omega_{2m} = (\phi_{c_t})_{2m}/(\phi_{c_t})_{2f} + (\phi_{c_t})_{2m} + (\phi_{c_t})_{2c}$
Elastic storability ratio of cavity system	$\omega_{2c} = (\phi_{c_t})_{2c}/(\phi_{c_t})_{2f} + (\phi_{c_t})_{2m} + (\phi_{c_t})_{2c}$

system, which is determined by elastic storability ratio of the matrix system or cavity system

- (3) This reservoir is circular, and the upper, lower, and horizontal boundaries are closed
- (4) The properties of rock (including matrix, cavity, and fracture), such as permeability and porosity, are constant and do not change with reservoir pressure
- (5) A vertical well is located in the middle of this compound reservoir model, and wellbore storage and skin effect are not considered in this model
- (6) Pure oil phase flow happens in this reservoir with constant compressibility and viscosity. Isothermal and Darcy flow are assumed in this compound model

**2.2. Establishment of Mathematical Model.** For the sake of simplicity to obtain a rate decline prediction model of AFVWs in pore-cavity-fracture carbonate reservoirs, the important dimensionless variables used in this study are defined in Table 1.

Where  $\alpha$  and  $\beta$  are the ratio of diffusivity and conductivity between natural fractures in the outer zone and acid-eroded fractures and wormholes in the inner zone, respectively. They reflect the relative strength of diffusivity and conductivity of the inner and outer zones, which depend

on acid fracturing process and reservoir properties.  $\lambda$  is the crossflow coefficient between any two media systems of the outer zone;  $\omega$  is the elastic storage capacity ratio of one medium system (including natural fracture, matrix, and cavity) in the outer zone and represents the proportion of crude oil reserves in this triple-continuum system, having an implicit relationship  $\omega_{2f} + \omega_{2m} + \omega_{2v} = 1$ .

**2.2.1. Mathematical Model of Seepage Flow in Inner Zone.** For an AFVW, the main seepage channels in the inner zone are acid-eroded fractures and wormholes. Assuming Darcy linear flow in these channels, the governing equation in the inner zone can be established.

$$\frac{3.6k_1}{\mu} \frac{\partial^2 p_1}{\partial r^2} = (\phi_{c_t})_1 \frac{\partial p_1}{\partial t}. \quad (1)$$

Initial reservoir pressure,  $p_i$ , is uniformly distributed in the reservoir. Assume this well produces at a constant flow rate and the total production of multiple artificial fracture or wormhole system is equal to the well productivity,  $q$ . Hence, the initial and wellbore flow conditions are given as

$$p_1(r, 0) = p_i \quad (0 \leq r \leq r_f), \quad (2)$$

$$N \cdot 0.0864bh \left. \frac{k_1}{\mu} \frac{\partial p_1}{\partial r} \right|_{r=0} = qB. \quad (3)$$

Through a series of nondimensionalization, the above equations can be simplified as follows:

$$\frac{\partial^2 p_{1D}}{\partial r_D^2} = \alpha \frac{\partial p_{1D}}{\partial t_D}, \quad (4)$$

$$p_{1D}(r_D, 0) = 0 \quad (0 \leq r_D \leq r_{fD}), \quad (5)$$

$$\left. \frac{\partial p_{1D}}{\partial r_D} \right|_{r_D=0} = -\beta. \quad (6)$$

**2.2.2. Mathematical Model of Seepage Flow Outer Zone.** The outer zone corresponds to a typical pore-cavity-fracture composite reservoir. According to the triple media model proposed by Liu et al. [6], pseudo-steady crossflow occurs in these triple media systems. The dimensionless governing equations of natural fractures, matrix pores, and cavities are:

$$\frac{\partial^2 p_{2fD}}{\partial r_D^2} + \frac{1}{r_D} \frac{\partial p_{2fD}}{\partial r_D} = \frac{\partial p_{2fD}}{\partial t_D} + \frac{\omega_{2m}}{\omega_{2f}} \frac{\partial p_{2mD}}{\partial t_D} + \frac{\omega_{2c}}{\omega_{2f}} \frac{\partial p_{2cD}}{\partial t_D}, \quad (7)$$

$$\frac{\omega_{2m}}{\omega_{2f}} \frac{\partial p_{2mD}}{\partial t_D} + \lambda_{mf} (p_{2mD} - p_{2fD}) - \lambda_{cm} (p_{2cD} - p_{2mD}) = 0, \quad (8)$$



TABLE 2: Coefficient of analytical solution of bottomhole pressure of AFVWs under different external boundary conditions (closed, constant pressure, and infinite).

External boundary condition	$x_2$	
	$x_1$	
Closed	$K_1(\sqrt{sh(s)}r_{eD})I_0(\sqrt{sh(s)}) + I_1(\sqrt{sh(s)}r_{eD})K_0(\sqrt{sh(s)})/I_1(\sqrt{sh(s)})$	$(\beta\sqrt{h(s)}/\sqrt{\alpha})\left(K_1(\sqrt{sh(s)}r_{eD}) - I_1(\sqrt{sh(s)}r_{eD})K_1(\sqrt{sh(s)})/I_1(\sqrt{sh(s)}r_{eD})\right)$
Constant pressure	$K_0(\sqrt{sh(s)}) - (K_0(\sqrt{sh(s)}r_{eD})/I_0(\sqrt{sh(s)}r_{eD}))I_0(\sqrt{sh(s)})$	$-(\beta\sqrt{h(s)}/\sqrt{\alpha})\left[K_1(\sqrt{sh(s)})/I_0(\sqrt{sh(s)}r_{eD}) + (K_0(\sqrt{sh(s)}r_{eD})/I_0(\sqrt{sh(s)}r_{eD}))I_1(\sqrt{sh(s)})\right]$
Infinite	$K_0(\sqrt{sh(s)})$	$-(\beta\sqrt{h(s)}/\sqrt{\alpha})K_1(\sqrt{sh(s)})$

where

$$\begin{aligned}
a_1 &= -\alpha \frac{\Delta^2 r_D}{\Delta t_D} - 2, b_1 = -2\beta \Delta r_D, a_2(i) \\
&= 1 - \frac{\Delta r_{D1}}{2[1 + (i - J - 1)\Delta r_{D1}]} \quad i = J + 1, J + 2 \dots I, \\
a_3 &= -\frac{\Delta r_{D1}^2}{\omega_{2f} \Delta t_D} \left[ \frac{\omega_{2m}(A\lambda_{mf} + \lambda_{cm}\lambda_{cf}) + \omega_{2c}(B\lambda_{cf} + \lambda_{cm}\lambda_{mf})}{AB - \lambda_{cm}^2} \right] \\
&\quad - \frac{\Delta r_{D1}^2}{\Delta t_D} - 2, \\
a_4(i) &= 1 + \frac{\Delta r_{D1}}{2[1 + (i - J - 1)\Delta r_{D1}]} i \\
&= J + 1, J + 2 \dots I; r_{Di} \\
&= 1 + (i - J - 1)\Delta r_{D1}, a_5 = -\frac{\Delta r_{D1}^2}{\Delta t_D}, \\
a_6 &= \frac{\omega_{2m} \Delta r_{D1}^2}{\omega_{2f} \Delta t_D} \left[ \frac{A\omega_{2m} + \lambda_{cm}\omega_{2c}}{\omega_{2f} \Delta t_D (AB - \lambda_{cm}^2)} - 1 \right], \\
a_7 &= \frac{\omega_{2c} \Delta r_{D1}^2}{\omega_{2f} \Delta t_D} \left[ \frac{B\omega_{2c} + \lambda_{cm}\omega_{2m}}{\omega_{2f} \Delta t_D (AB - \lambda_{cm}^2)} - 1 \right], \\
a_8 &= \beta \frac{\Delta r_D}{\Delta r_{D1}}, a_9 = 2 + \frac{a_3 a_8}{a_2 (J + 1)}, \\
a_{10} &= -a_8 \left( \frac{a_4 (J + 1)}{a_2 (J + 1)} + 1 \right), a_{11} = \frac{a_5 a_8}{a_2 (J + 1)}, \\
a_{12} &= -\frac{a_6 a_8}{a_2 (J + 1)}, a_{13} = -\frac{a_7 a_8}{a_2 (J + 1)}, \\
A &= \lambda_{cm} + \lambda_{cf} + \frac{\omega_{2c}}{\omega_{2f} \Delta t_D}, \\
B &= \lambda_{mf} + \lambda_{cm} + \frac{\omega_{2m}}{\omega_{2f} \Delta t_D}.
\end{aligned} \tag{19}$$

Finally, the virtual mirror grid method is used to deal with the internal and external boundary conditions and interface continuity conditions (Figure 4) [25, 26]. The different forms of the initial conditions of the inner and outer zones are:

$$p_i^0 = 0 \quad i = 1, 2, \dots, J, \tag{20}$$

$$f_i^0 = v_i^0 = m_i^0 = 0 \quad i = J + 1, J + 2, \dots, I. \tag{21}$$

Combined with Equations (19)–(21), a program is written to solve the above tridiagonal matrix by using the principle of catch-up method, and the numerical solution of bottomhole pressure under constant flow rate for an AFVW in a pore-cavity-fracture carbonate reservoir can be achieved. This numerical solution is an attempt to pursue faster computing speed.

### 3. Comparison between Analytical Solution and Numerical Solution of Bottomhole Pressure for an AFVW in a Pore-Cavity-Fracture Carbonate Reservoir

Figure 5 shows the comparison of analytical solution and numerical solution, including bottomhole pressure and pressure derivative, for an AFVW in a compound reservoir model under different parameters. Obviously, the analytical solution is basically consistent with the numerical solution in the whole production period for different interzonal diffusivity ratios, interzonal conductivity ratios, elastic storability ratios, and crossflow coefficients. A slight deviation of pressure derivative can be observed in locally short production stage, but within an acceptable range. Therefore, our algorithms of analytical solution and numerical solution of bottomhole pressure are reliable. In terms of computational efficiency, the computing speed of numerical solution is indeed faster than that of analytical solution, but the analytical solution is easier to deal with wellbore storage and skin and is also easier to extend to the study of unstable productivity. Overall, the analytical solution and numerical solution for this compound model have their own advantages in well testing.

### 4. Conventional Rate Decline and Cumulative Productivity for an AFVW in a Pore-Cavity-Fracture Carbonate Reservoir

Considering wellbore storage and skin damage, the analytical solution of bottomhole pressure under constant rate of an AFVW can be written as [27].

$$\tilde{p}_{swD}(C_D, S, s) = \frac{\tilde{s} \tilde{p}_{wD}(s) + S}{s[1 + C_D s(S + \tilde{s} \tilde{p}_{wD}(s))]}, \tag{22}$$

where  $C_D$  and  $S$  are wellbore storage coefficient and skin factor, respectively.

According to Duhamel's principle, there is a specific relationship between the bottomhole pressure under constant flow rate and the flow rate under constant bottomhole pressure in Laplace space [28], and then the instantaneous flow rate under constant bottomhole pressure of an AFVW can be got:

$$\tilde{q}_{wD}(C_D, S, s) = \frac{1}{s^2 \tilde{p}_{swD}(C_D, S, s)}. \tag{23}$$

Furthermore, based on the relationship between instantaneous rate and cumulative productivity, the cumulative productivity under constant bottomhole pressure of an AFVW can be obtained:

$$\tilde{q}_{cD}(C_D, S, s) = \frac{\tilde{q}_{wD}(C_D, S, s)}{s}. \tag{24}$$

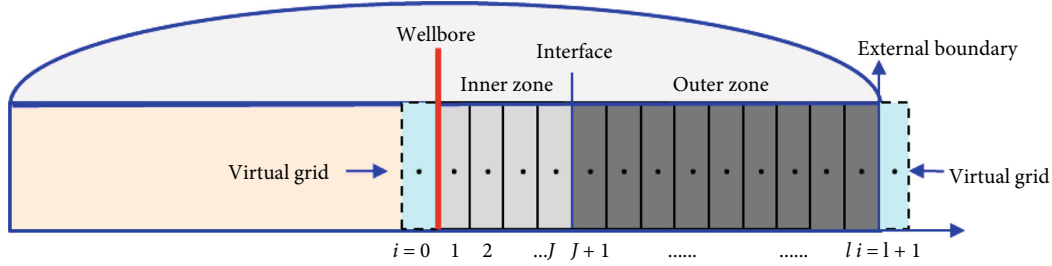


FIGURE 4: Discrete grid diagram of circular compound reservoir.

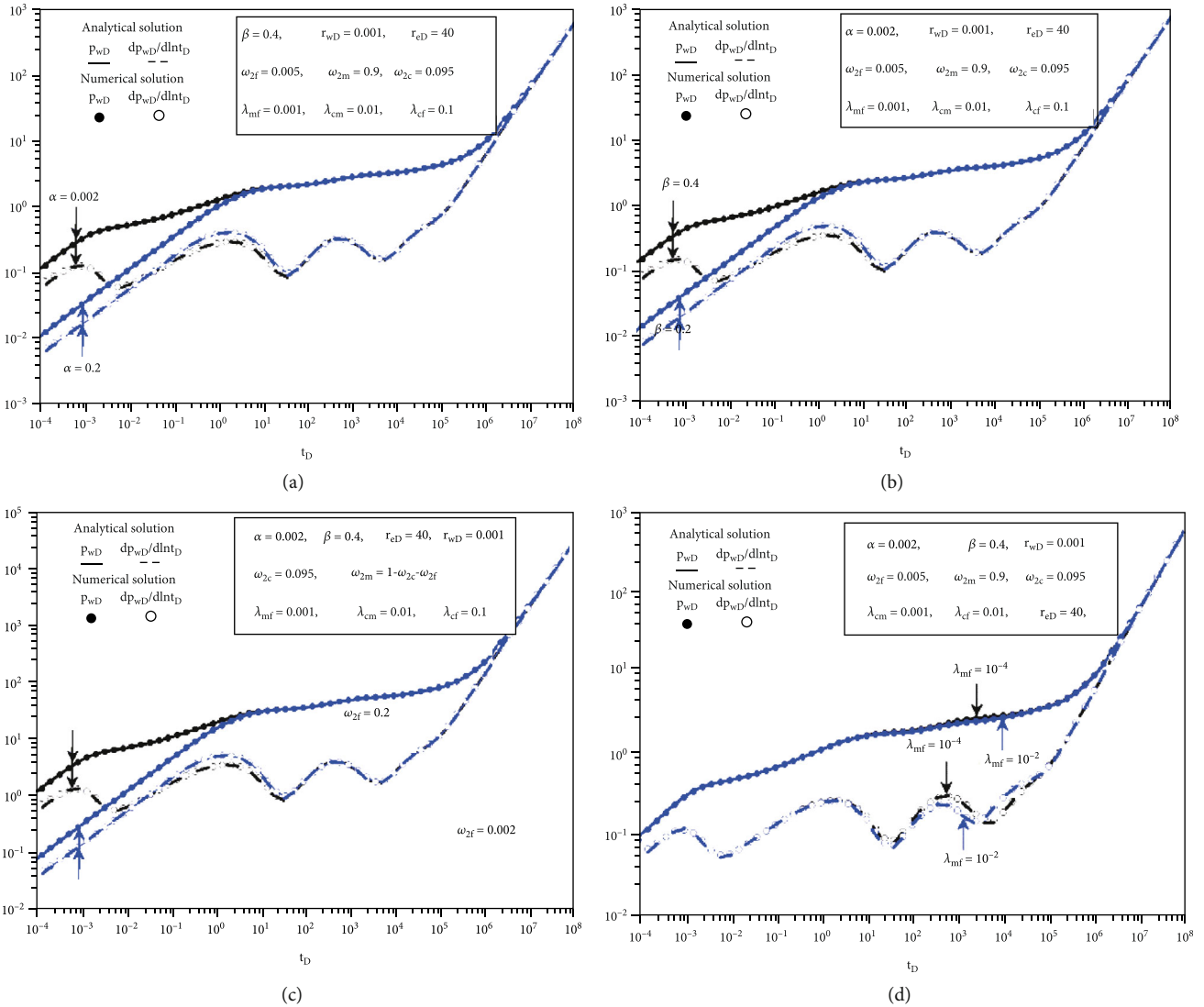


FIGURE 5: Comparison of analytical solution and numerical solution of bottomhole pressure in a compound reservoir model under different parameters ((a) interzonal diffusivity ratio: 0.002, 0.2; (b) interzonal conductivity ratio: 0.2, 0.4; (c) elastic storability ratio of natural fracture system: 0.002, 0.2; (d) matrix–fracture crossflow coefficient:  $10^{-4}$ ,  $10^{-2}$ ).

The research on the impact of wellbore storage and skin damage on well production has been very mature [27], which will not be discussed in this study. In order to facilitate this study, let  $C_D=0$  and  $S=0$ .

4.1. Production Comparison between Acid-Fracturing Well and Non-Acid-Fracturing Well in a Pore-Cavity-Fracture Carbonate Reservoir. Interzonal diffusivity ratio and interzonal conductivity ratio are not involved in the non-acid-



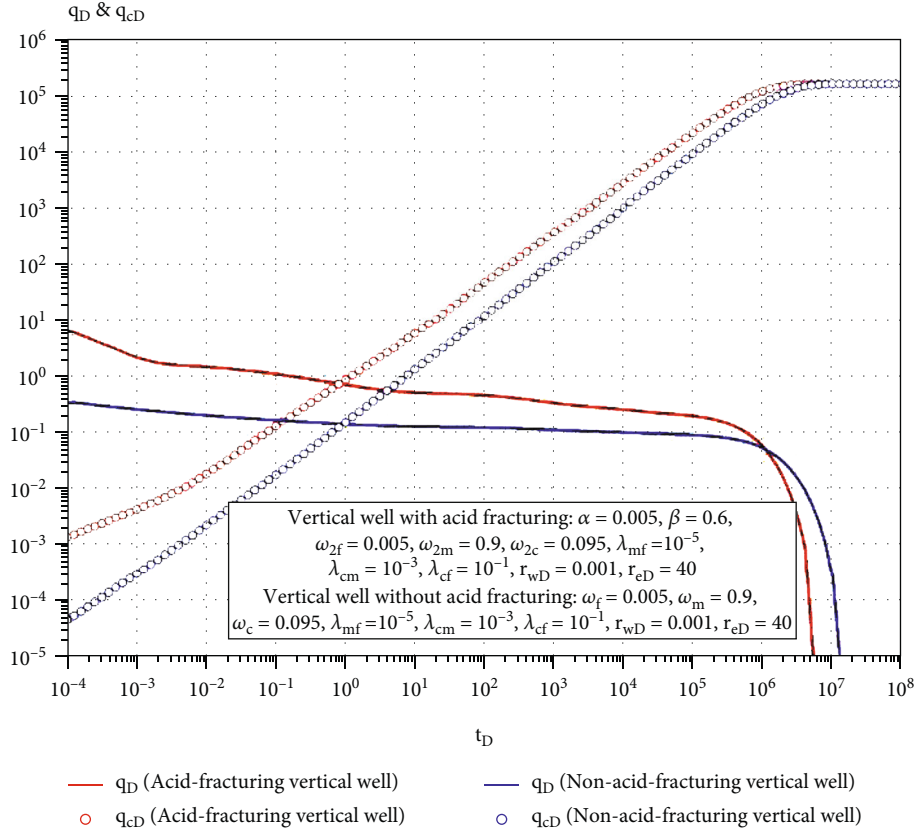


FIGURE 6: Comparison of instantaneous rate and cumulative productivity between acid-fracturing vertical well and non-acid-fracturing vertical well.

fracturing vertical well model. Figure 6 shows the comparison of instantaneous rate and cumulative productivity between acid-fracturing vertical well and non-acid-fracturing vertical well under the same reservoir properties. In the early- and middle-production period, both the instantaneous rate and cumulative productivity of acid-fracturing vertical well are higher than those of non-acid-fracturing vertical well, but the production of acid-fracturing well decreases faster. In the late-production period, the instantaneous rates of two vertical wells exhibit the opposite trend, but the difference can be neglected considering the low productivity in this period. However, the cumulative productivity of two vertical wells is gradually close in the late stage, revealing that acid fracturing mainly increases the early production but has little effect on the final cumulative production if production time is not taken into account. Acid fracturing is often used to improve the early well productivity in order to improve production efficiency, quickly recover investment, and maximize economic value.

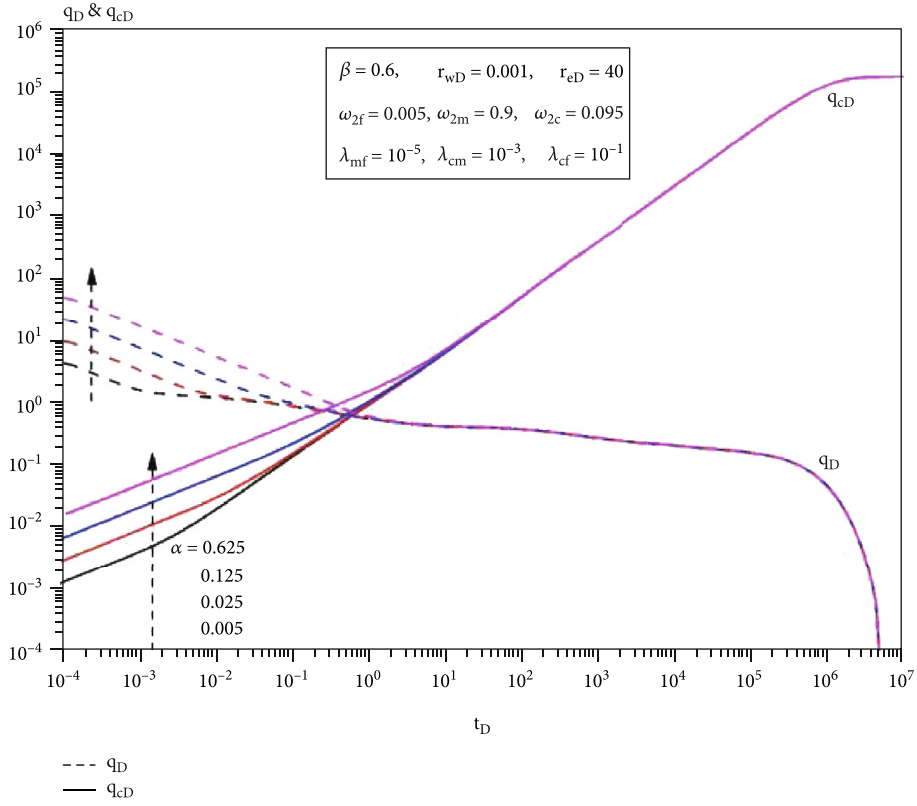
#### 4.2. Sensitivity Analysis of Production of an AFVW in a Pore-Cavity-Fracture Carbonate Reservoir

4.2.1. *Interzonal Diffusivity Ratio and Interzonal Conductivity Ratio.* Figures 7(a) and 7(b) present the production behavior of an AFVW under different interzonal diffusivity ratios and interzonal conductivity ratios, respectively. Three typical production stages can be observed for

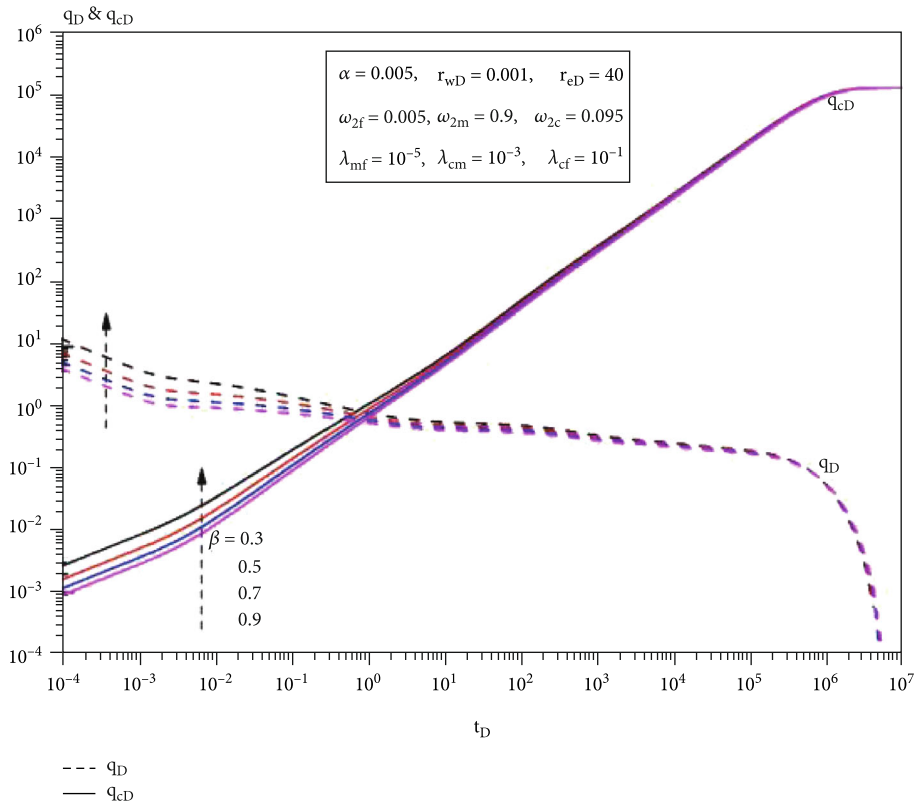
an AFVW, including early linear decline stage (oil supplied by acid-eroded fractures and wormholes), middle stable production stage, and late decline stage. Interzonal diffusivity ratio and interzonal conductivity ratio mainly affect the early production. A greater interzonal diffusivity ratio, meaning a stronger fracture diffusivity in the outer zone, leads to a higher early productivity, while a larger interzonal conductivity ratio, meaning a weaker fracture conductivity in the inner zone, leads to a lower early productivity. Meanwhile, interzonal diffusivity ratio has a shorter impact on the well production than interzonal conductivity ratio. However, in the late stage, the instantaneous rate and cumulative productivity are very close, respectively. Considering that the above two ratios depend on acid fracturing operation, it seems to suggest that acid fracturing has little influence on the final productivity. On the contrary, this proves that acid fracturing only works for a certain period of time, which is in line with the field requirement of rapid cost recovery and high production efficiency. Hence, it is necessary to optimize these two ratios to improve early productivity before conducting acid fracturing.

#### 4.2.2. Elastic Storability Ratios of Triple Media Reservoir.

Figures 8(a)–8(c) show the influence of elastic storability ratios of three kinds of media on the production of an AFVW, respectively. The comparison shows that the production performance for different elastic storability ratios of matrix system and cavity system (Figures 8(b) and 8(c))

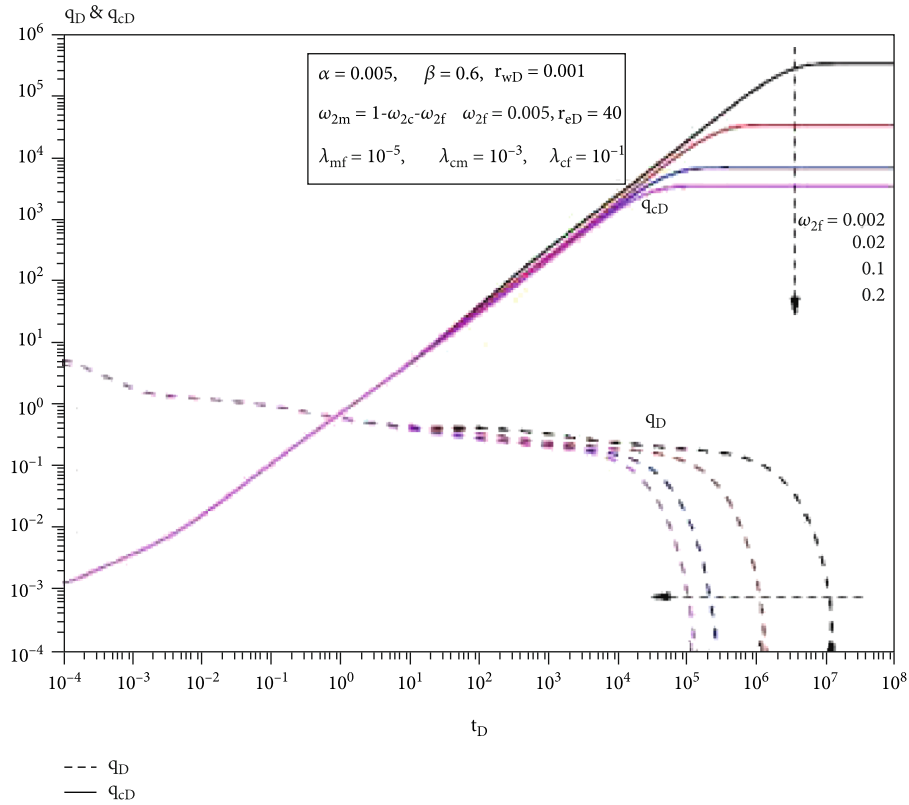


(a) Interzonal diffusivity ratio

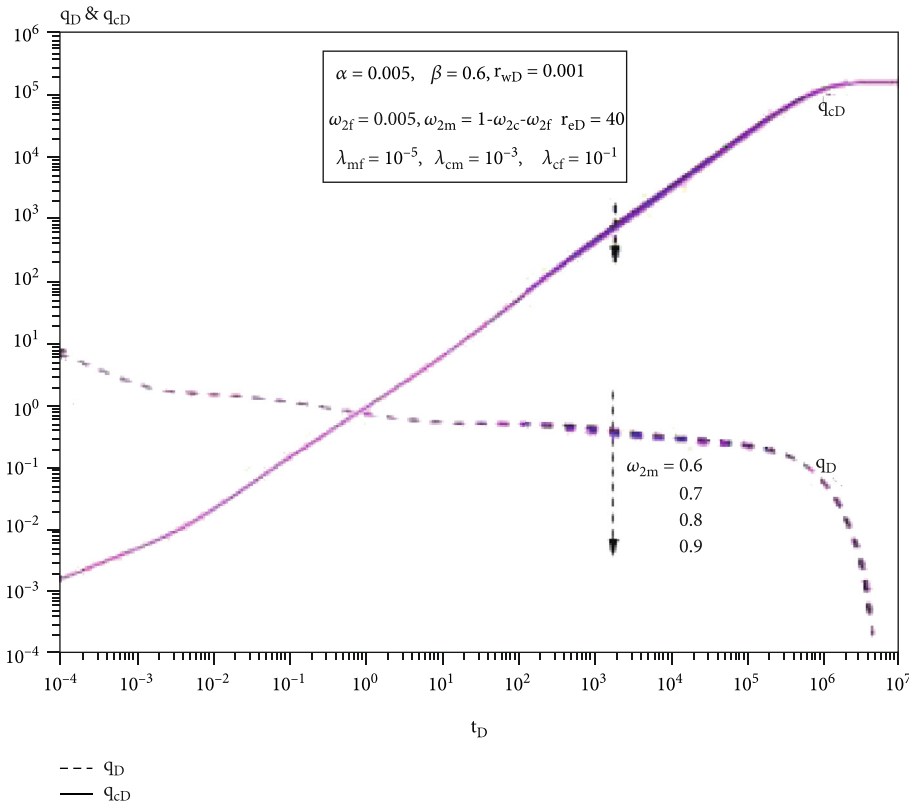


(b) Interzonal conductivity ratio

FIGURE 7: Influence of interzonal diffusivity ratio and interzonal conductivity ratio on the production of an AFVW in a pore-cavity-fracture carbonate reservoir.

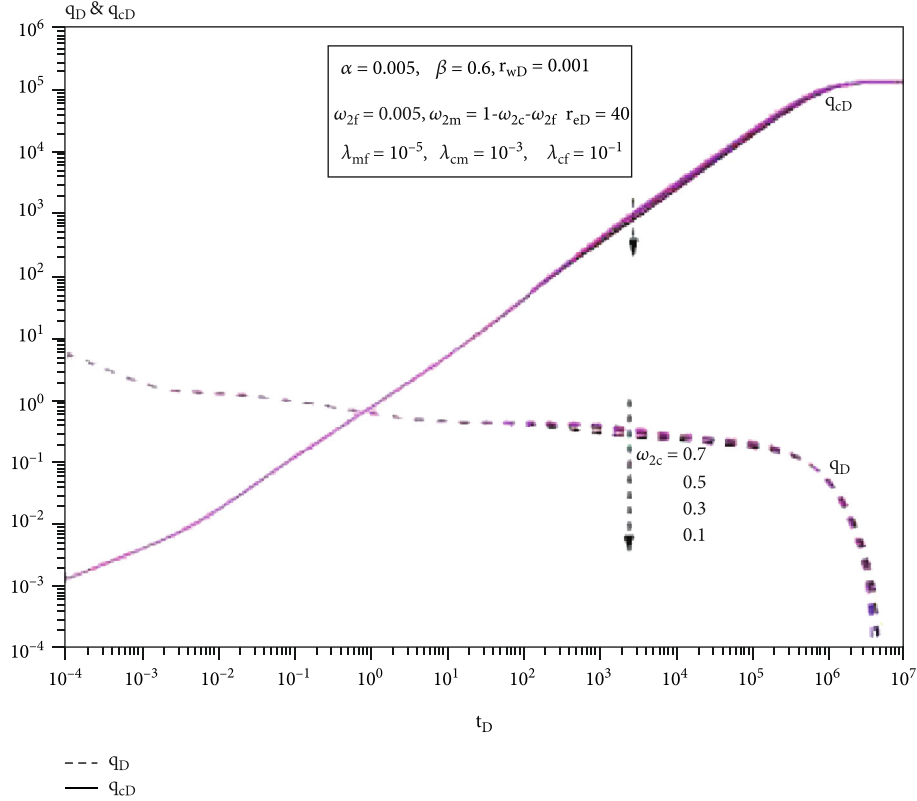


(a) Elastic storability ratio of natural fracture system



(b) Elastic storability ratio of matrix system

FIGURE 8: Continued.



(c) Elastic storability ratio of cavity system

FIGURE 8: Influence of elastic storability ratios of triple media on the production of an AFVW in a pore-cavity-fracture carbonate reservoir.

nearly coincide in the whole period, and only a slight difference occurs in the middle period, indicating that when the elastic storability ratio of natural fracture system remains unchanged, the other two ratios have weak impact on well production. Storability ratio of natural fracture system strongly affects the late productivity, and the depletion decline stage appears earlier when this ratio increases gradually (Figure 8(a)). Considering the implicit relationship,  $\omega_{2f} + \omega_{2m} + \omega_{2v} = 1$ , it can be interpreted by that the increase of natural fractures' elastic storability ratio diminishes the storability of the other two systems and thus weakens the supply capacity of matrix and cavity in the late stage and results in the advance of depletion decline stage.

#### 4.2.3. Crossflow Coefficients of Triple Media Reservoir.

Figures 9(a)–9(c) demonstrate that in a pore-cavity-fracture carbonate reservoir, the production performances of an AFVW under different crossflow coefficients are very close on the whole. There are slight production differences at some specific periods, indicating that crossflow coefficient has weak effect on the instantaneous rate and cumulative productivity of acid fracturing vertical wells, but this slight difference is not conducive to parameter inversion in well test.

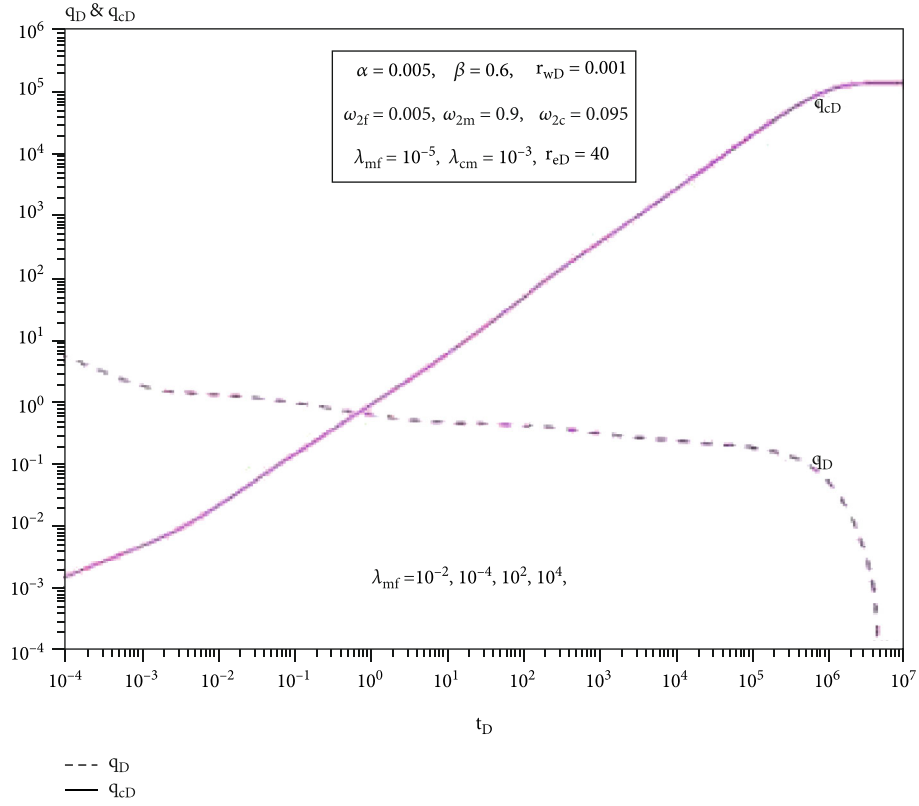
4.2.4. Compound Reservoir Radius. Figure 10 displays the production behavior of an AFVW under different reservoir radius. For a closed reservoir, in the early producing period,

the bottomhole pressure drop does not affect the external reservoir boundary and the instantaneous rate and cumulative productivity are the same, respectively. However, the well productivity begins to diverge when the pressure drop reaches the external boundary in the late period. When reservoir radius decreases, the depletion decline stage appears earlier and also the final cumulative productivity gets lower, which is the same as the production behavior of other closed reservoirs and helpful to determine reservoir radius in well test.

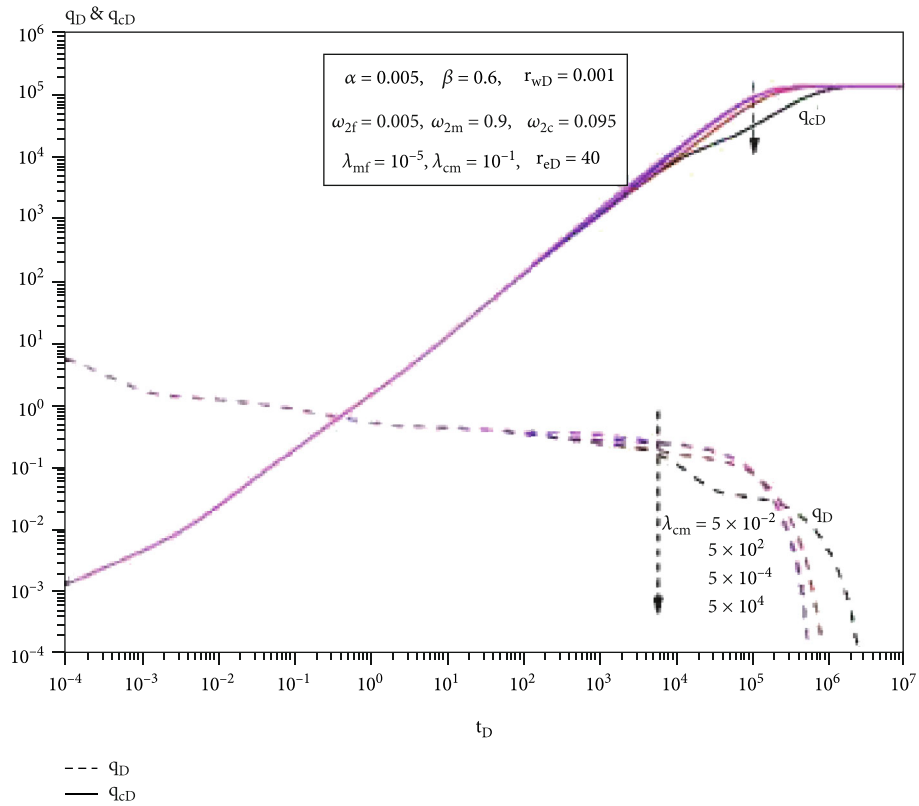
## 5. New Type Rate Decline Curves for an AFVW in a Pore-Cavity-Fracture Carbonate Reservoir

When using conventional rate decline curves in Figures 8 or 9 to inverse reservoir parameters, multiple solutions are likely to appear in well-test inversion. Fetkovich and Blasingame established new type rate decline curves to reduce the possibility of multiple solutions by defining material balance time [29, 30]. Moreover, Blasingame type rate decline curves have advantages in dealing with the problems of variable bottomhole pressure and variable flow rate, which is closer to the actual situation [30].

Pseudo-steady flow always happens in the late-production period for an AFVW in a closed compound

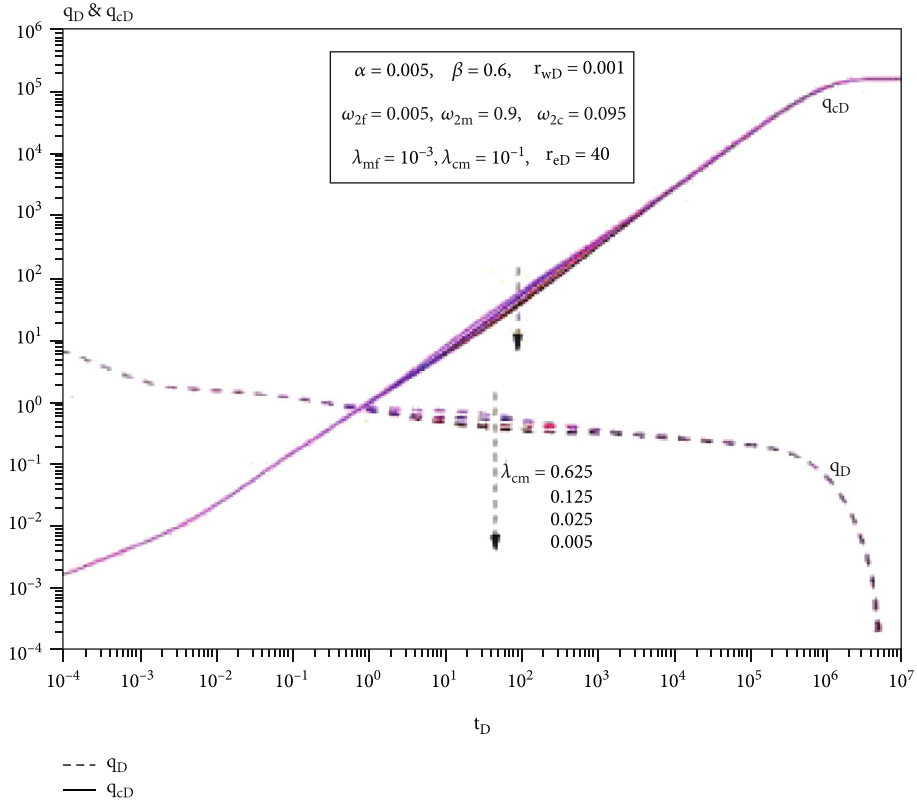


(a) Matrix-fracture crossflow coefficient



(b) Cavity-matrix crossflow coefficient

FIGURE 9: Continued.



(c) Cavity-fracture crossflow coefficient

FIGURE 9: Influence of crossflow coefficients of triple media on the production of an AFVW in a pore-cavity-fracture carbonate reservoir.

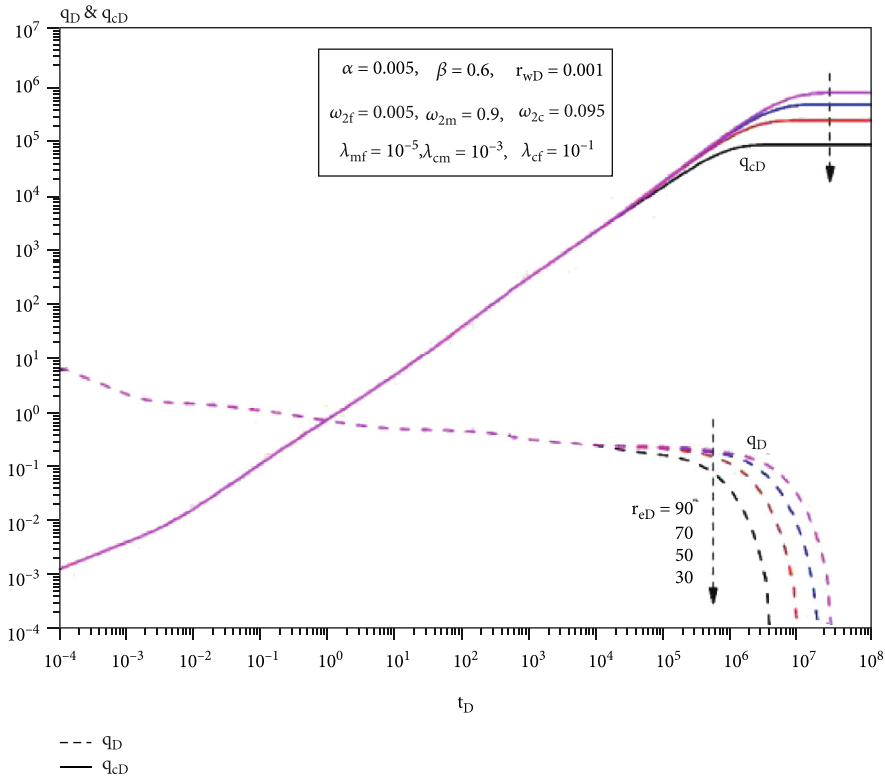


FIGURE 10: Influence of reservoir radius on the production of an AFVW in a pore-cavity-fracture carbonate reservoir.

reservoir. With the progressive analysis method, the analytical solution of bottomhole pressure (Equation (14)) in Laplace space can be simplified to (when  $s$  approaches 0)

$$p_{wD,ps}(s) \approx \frac{2\omega_{2f}}{r_{eD}^2 - 1} \frac{1}{s^2} + \left[ \frac{1}{2(r_{eD}^2 - 1)} + \frac{((\ln \omega_{2f}/2) + \ln 2 - 0.5772)r_{eD}^2}{r_{eD}^2 - 1} \right] \frac{1}{s} - \frac{r_{eD}^2}{2(r_{eD}^2 - 1)} \frac{\ln s}{s}. \quad (25)$$

Through Laplace inverse transformation (when production time approaches infinity), the approximate analytical solution of bottomhole pressure in the late-production period can be obtained in real space:

$$p_{wD,ps}(t_D) = \frac{2\omega_{2f}t_D}{(r_{eD}^2 - 1)} + \frac{r_{eD}^2 \ln(\omega_{2f}t_D)}{2(r_{eD}^2 - 1)} + \frac{r_{eD}^2(\ln 4 - 0.5772) + 1}{2(r_{eD}^2 - 1)}. \quad (26)$$

Furthermore, combined with the characteristics of pseudo-steady-state flow, the following pseudo-steady constant [29] can be defined:

$$b_{Dps} = \frac{r_{eD}^2(\ln 4 - 0.5772) + 1}{2(r_{eD}^2 - 1)}. \quad (27)$$

Referring to the rate decline curves developed by Fetkovich and Blasingame, the following new rate functions can be defined [29, 30].

$$t_{Dd} = \frac{2}{b_{Dps}(r_{eD}^2 - 1)} t_D, \quad (28)$$

$$q_{Dd} = q_D b_{Dps}, \quad (29)$$

$$q_{Ddi} = \frac{N_{pDd}}{t_{Dd}} = \frac{1}{t_{Dd}} \int_0^{t_{Dd}} q_{Dd}(\tau) d\tau, \quad (30)$$

$$q_{Ddid} = -\frac{dq_{Ddi}}{d \ln(t_{Dd})} = -t_{Dd} \frac{dq_{Ddi}}{dt_{Dd}} = q_{Ddi} - q_{Dd}, \quad (31)$$

where  $t_{Dd}$  is material balance time,  $q_{Ddi}$  is rate integral function and  $q_{Ddid}$  is rate integral derivative function.

Taking  $t_{Dd}$  as the horizontal axis and  $q_{Ddi}$  and  $q_{Ddid}$  as the vertical axis and adopting the double-logarithmic coordinates, a kind of new type rate decline curves can be established for an AFVW in a pore-cavity-fracture carbonate reservoir.

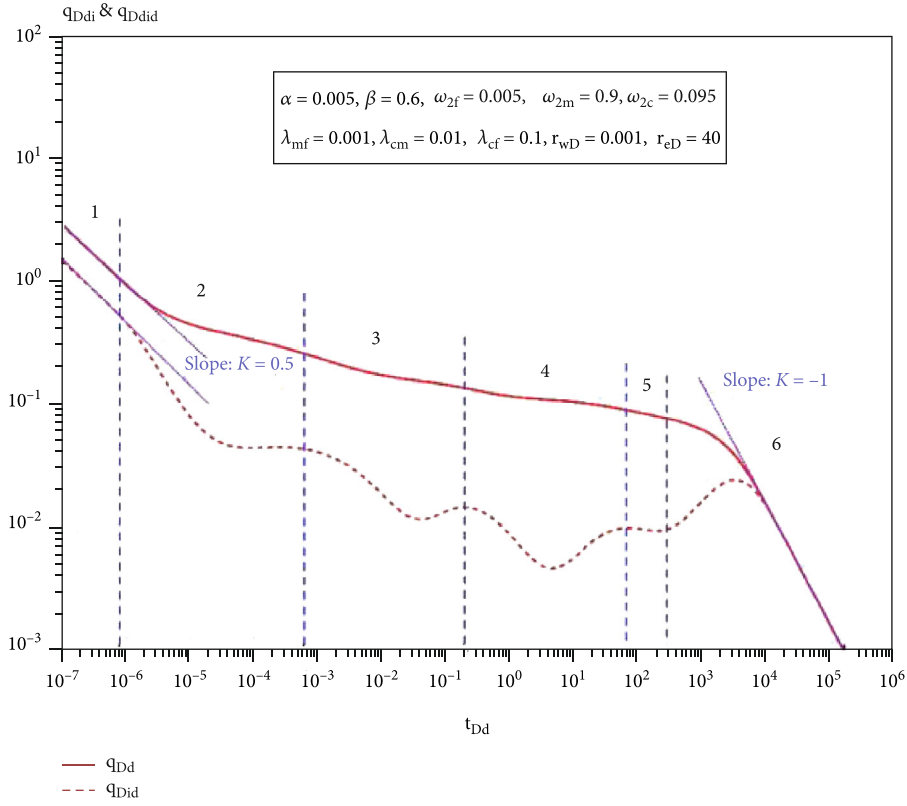
**5.1. Identification of Typical Flow Regimes.** In actual oil fields, the reserve of pore-cavity-fracture carbonate reser-

voirs can be dominated by matrix system or cavity system. The former is represented by some carbonate reservoirs in Middle East and Central Asia, and the latter is represented by fracture-cavity reservoirs in Tarim Oilfield. Figures 11(a) and 11(b) show the flow regime identification on the new rate decline curves for an AFVW in a pore-cavity-fracture carbonate reservoir under different reserve dominant types, respectively.

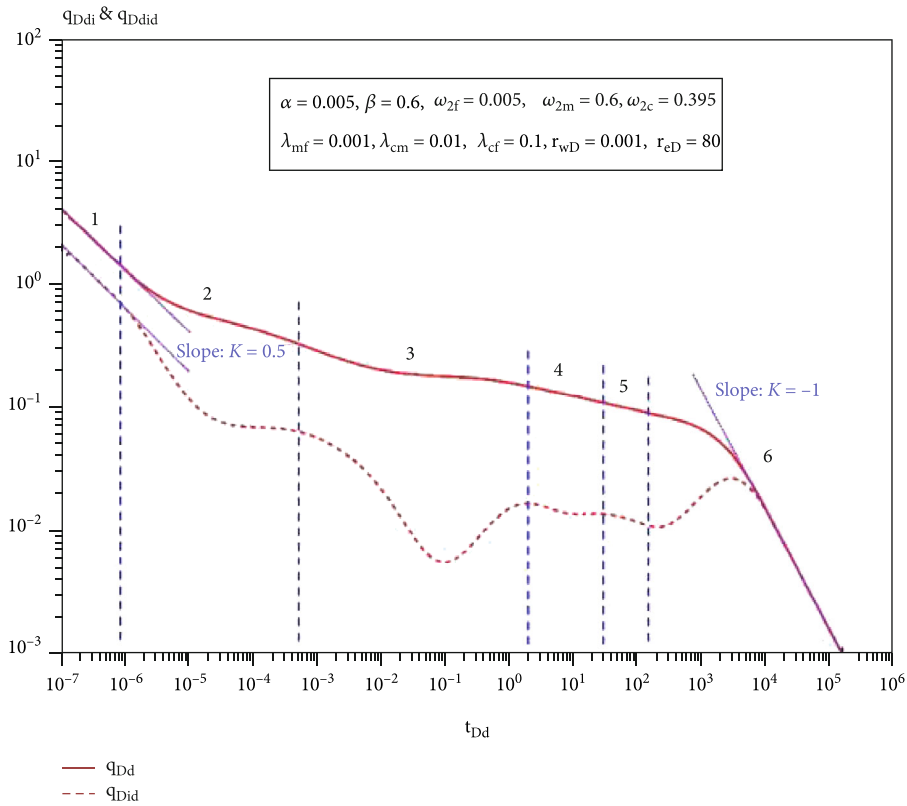
For carbonate reservoirs with reserves dominated by matrix system, six typical flow regimes can be identified in the whole production period (Figure 11(a)).

- (1) Acid-eroded fracture and wormhole linear flow regime: at the starting of well production, the crude oil in acid-eroded fractures and wormholes preferentially flows into the wellbore. The curves of rate integral function and rate integral derivative function are characterized by a pair of parallel falling straight lines with a slope of -0.5
- (2) Interzonal transition flow regime: when the pressure wave spreads to the interface, the transition flow between the inner and outer zone appears. A V-segment appears on the curve of rate integral derivative function
- (3) Cavity-fracture crossflow regime: a part of cavities directly connects with natural fractures, and the crude oil in these cavities flows into natural fractures first when the pressure in natural fracture system drops, and the second V-segment appears on the curve of rate integral derivative function
- (4) Matrix-fracture and cavity-matrix crossflow regime: as the pressure in the cavity system decreases, the crude oil in the matrix system begins to flow into natural fractures. Furthermore, when the pressure in the matrix system drops, the crude oil in the cavities which do not connect with natural fractures begins to flow into the matrix system. These two crossflows lead to the third V-segment on the curve of rate integral derivative function
- (5) Pseudo-radial flow regime: when the pressure drop area expands, the crossflows among the triple media system gradually reach a dynamic balance, and pseudo-radial flow appears in the reservoir. The curve of rate integral derivative function is characterized by a horizontal straight line
- (6) Pseudo-steady flow regime: when the pressure wave reaches the external reservoir boundary, pseudo-steady flow appears and the curves of rate integral function and rate integral derivative function converge into a straight line with a slope of -1

For carbonate reservoirs whose reserves are dominated by cavity system, six typical flow regimes can also be identified on the new type curves (Figure 11(b)). The main difference between two reserve dominant types lies in the different characteristics of the new rate decline curves during the



(a) Carbonate reservoir dominated by matrix system



(b) Carbonate reservoir dominated by cavity system

FIGURE 11: Identification of typical flow regimes of new rate decline curves of an AFVW in a pore-cavity-fracture carbonate reservoir.



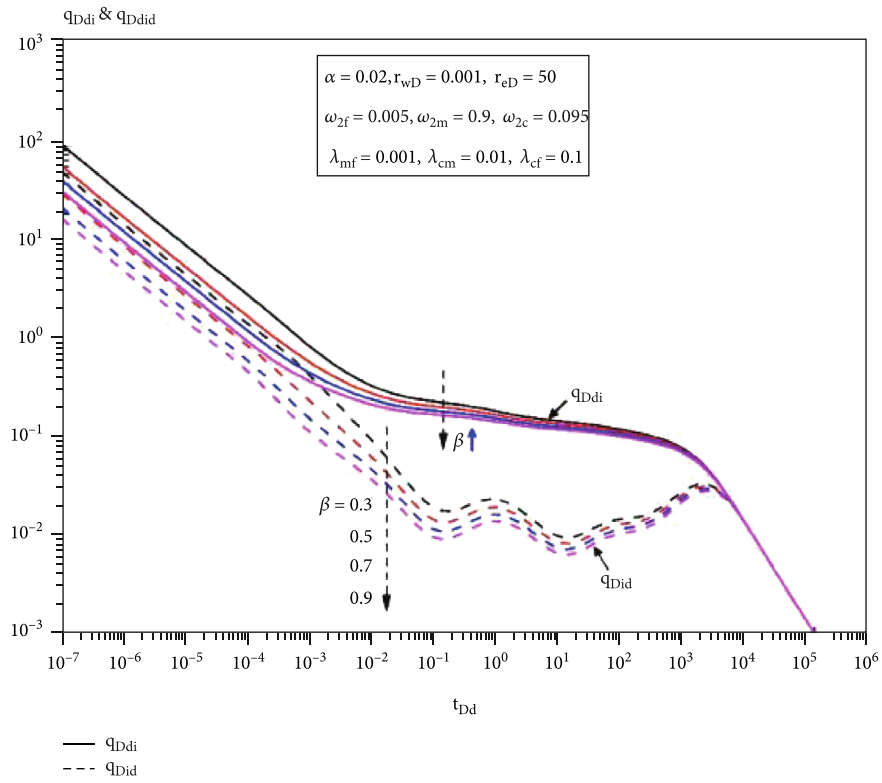
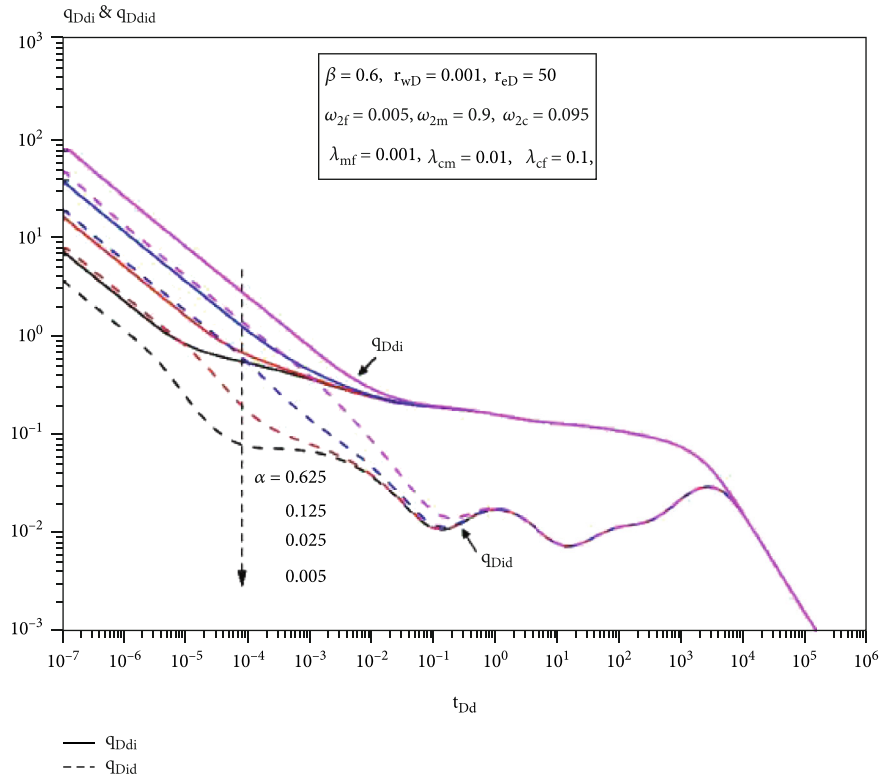


FIGURE 12: New rate decline curves of an AFVW in a pore-cavity-fracture carbonate reservoir under different interzonal diffusivity ratios and interzonal conductivity ratios.

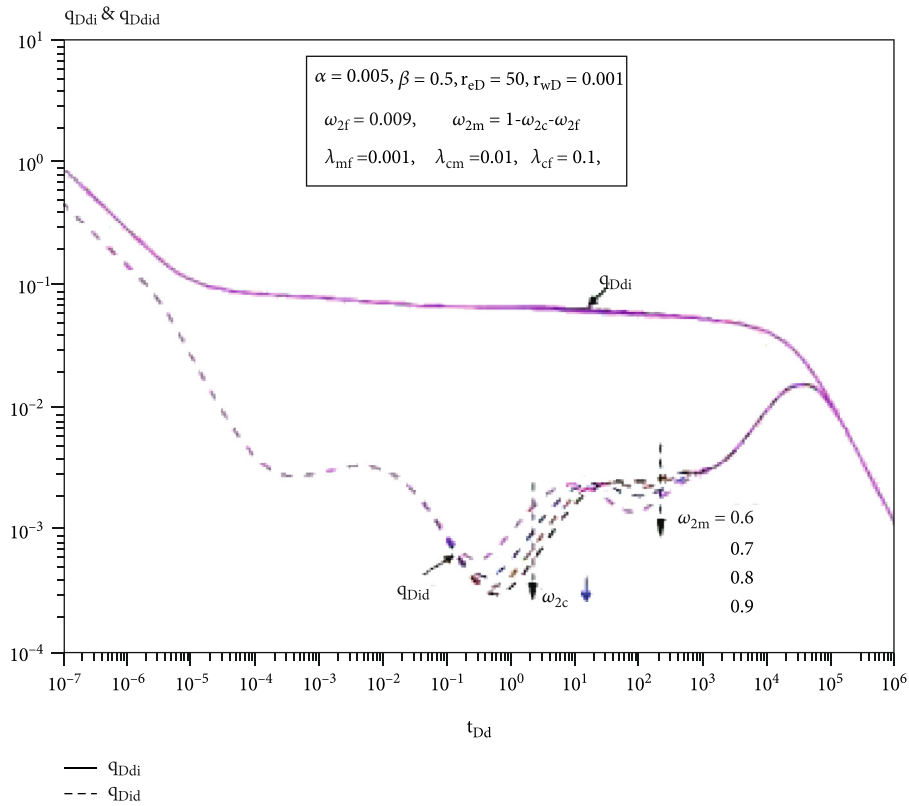
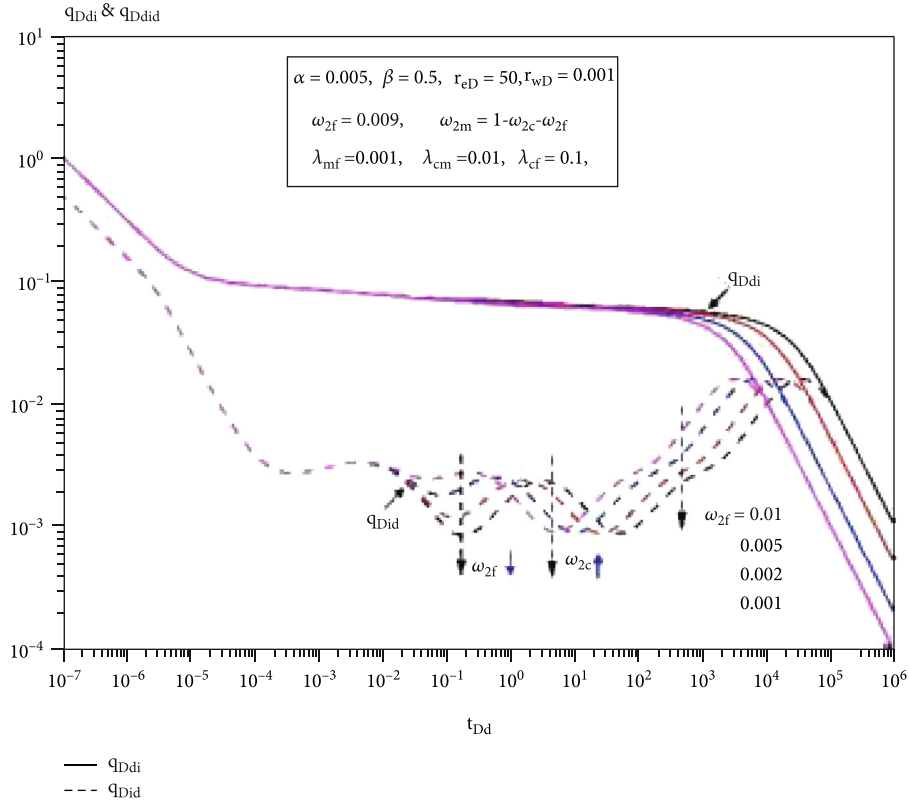
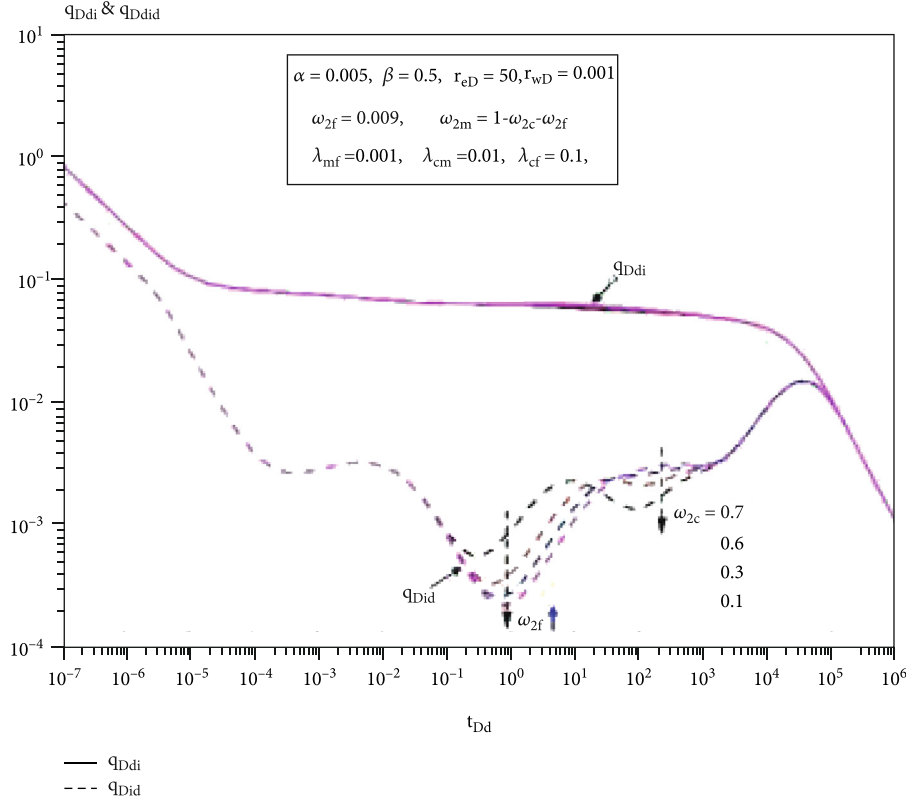


FIGURE 13: Continued.



(c) Elastic storability ratio of cavity system

FIGURE 13: New rate decline curves of an AFVW in a pore-cavity-fracture carbonate reservoir under different elastic storability ratios.

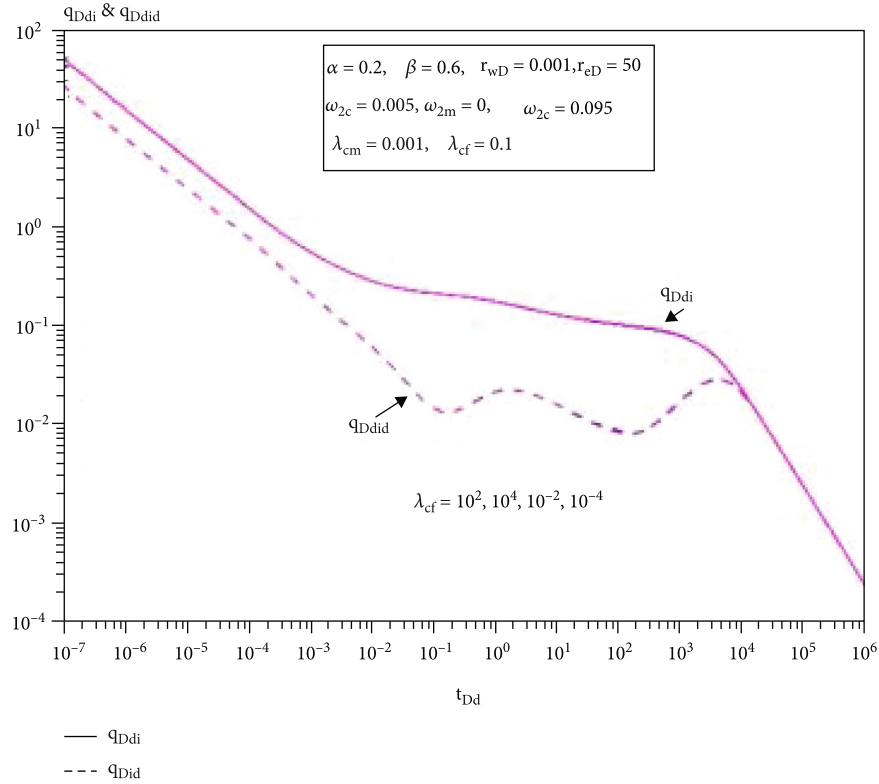
crossflow stage. The carbonate reservoir dominated by the cavity system only has one V-segment (corresponding to cavity-fracture crossflow regime) in the production period, but this regime lasts longer.

5.2. Sensitivity Analysis of New Rate Decline Curves of an AFVW in a Pore-Cavity-Fracture Carbonate Reservoir. Figures 12–15 shows the new type rate decline curves of an AFVW in a pore-cavity-fracture carbonate reservoir under different influencing factors. Compared with the conventional rate decline curves, the curve characteristics under different parameters are more significant and easier to be recognized, which is conducive to improving the accuracy and efficiency of well-test interpretation.

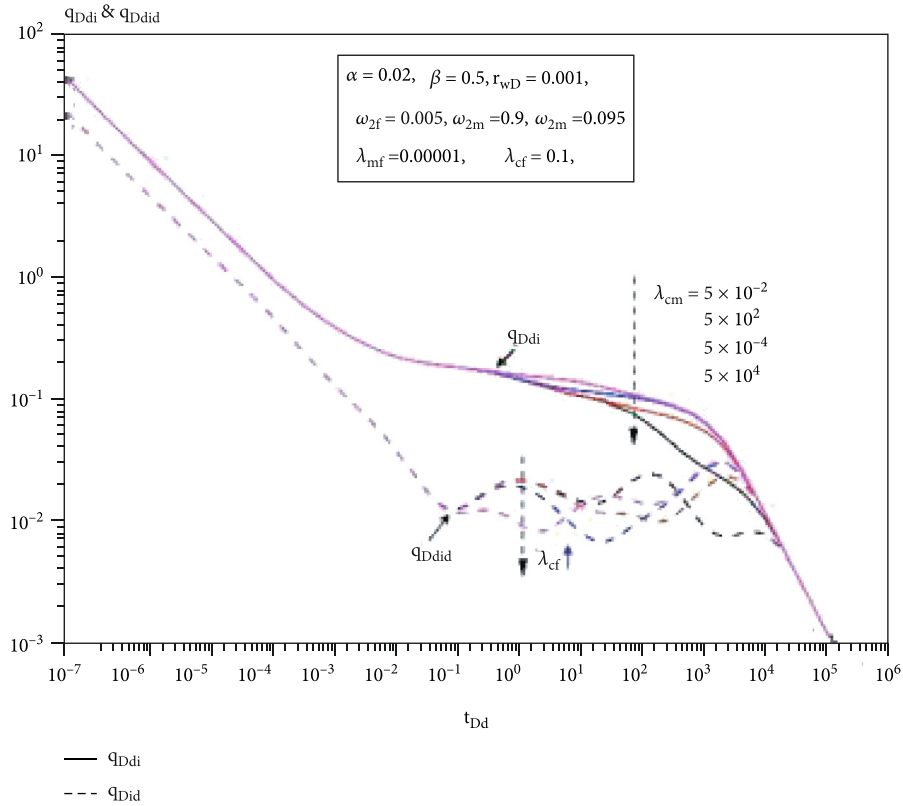
5.2.1. Interzonal Diffusivity Ratio and Interzonal Conductivity Ratio. Figure 12(a) presents the new type rate decline curves of an AFVW under different interzonal diffusivity ratios. Obviously, this ratio mainly affects two regimes, including acid-eroded fracture and wormhole linear flow regime and interzonal transition flow regime. As this diffusivity ratio decreases, both the rate integral and rate integral derivative before the crossflow regimes become lower, and the linear flow regime lasts shorter or even disappears, but the interzonal transition flow regime lasts longer. Figure 12(b) displays the new type rate decline curves under different interzonal conductivity ratios. All typical flow regimes except pseudo-steady flow regime are seri-

ously affected by the conductivity ratio. When this ratio gets low, both the rate integral and rate integral derivative become higher, the linear flow regime lasts longer, and the interzonal transition flow regime gets shorter. For different interzonal diffusivity and conductivity ratios, both the rate integral and rate integral derivative curves are completely normalized during the pseudo-steady flow regime.

5.2.2. Elastic Storability Ratios of Triple Media Reservoir. Figures 13(a)–13(c) demonstrate the new rate decline curves of an AFVW under different elastic storability ratios of triple media reservoir, respectively. The comparison shows that the elastic storability ratios of matrix and cavity only affect the crossflow regimes, but the elastic storability ratio of natural fracture also affects pseudo-steady flow regime, which is determined by elastic storability ratio and supply capacity of each system. The lower the elastic storability ratio of natural fracture system is, the deeper the second V-segment is and the longer the corresponding flow regime lasts, and then the occurrence of subsequent flow regime delays (Figure 13(a)). When the elastic storability ratio of matrix system decreases, the trend (depth and duration) of the second V-segment is the same as that affected by the elastic storability ratio of natural fracture system, but the third V-segment gets shallower and also the corresponding flow regime lasts shorter (Figure 13(b)). As the elastic storability ratio of cavity system drops, the second V-segment becomes shallower and the duration of the corresponding flow regime



(a) Matrix-fracture crossflow coefficient



(b) Cavity-matrix crossflow coefficient

FIGURE 14: Continued.

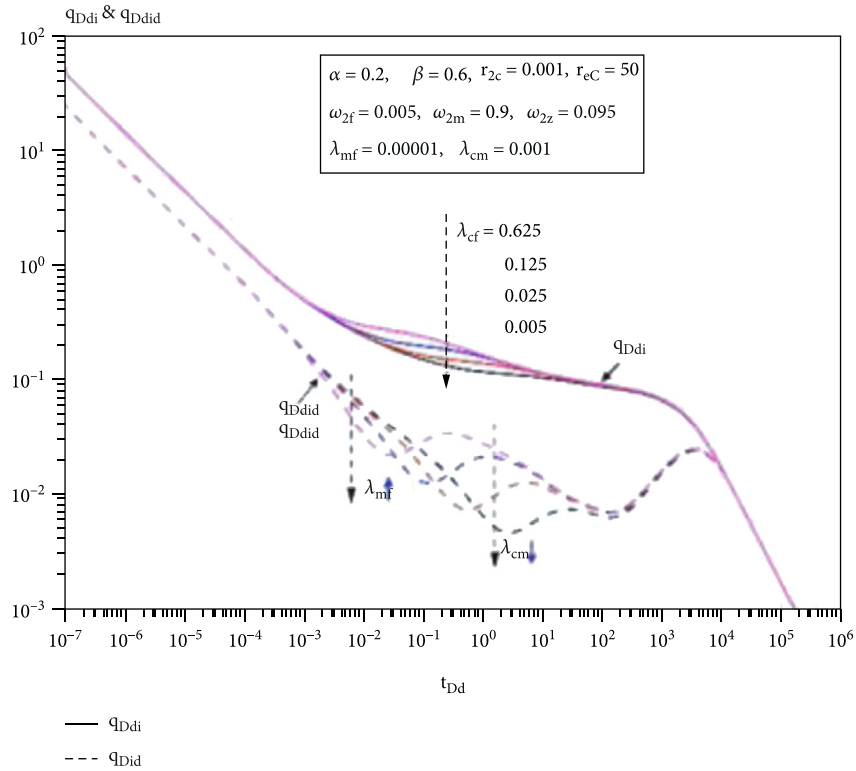


FIGURE 14: New rate decline curves of an AFVW in a pore-cavity-fracture carbonate reservoir under different crossflow coefficients.

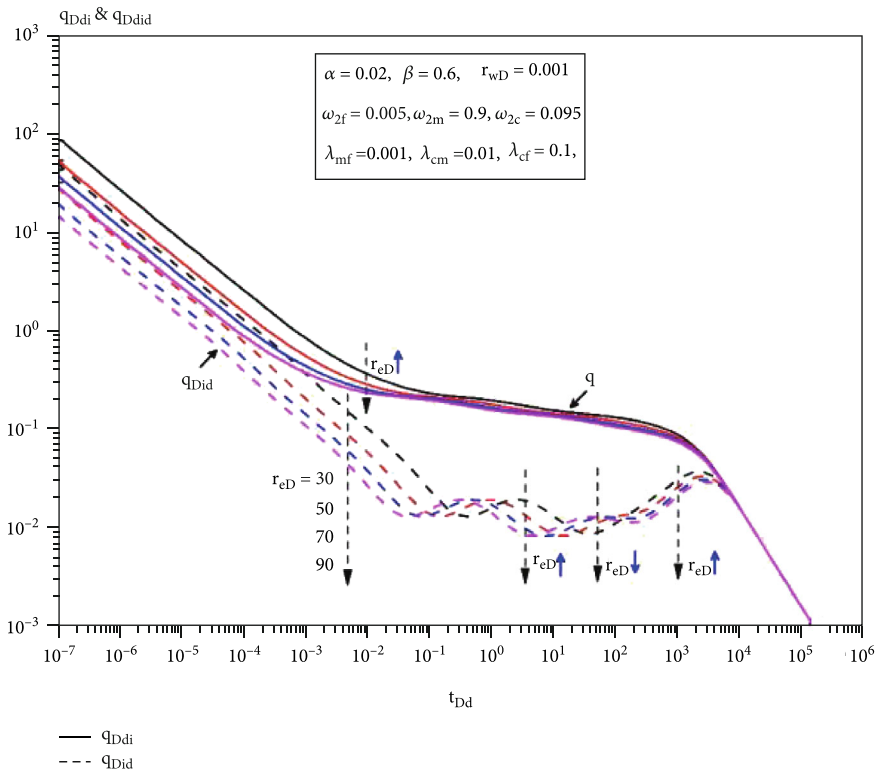


FIGURE 15: New rate decline curves of an AFVW in a pore-cavity-fracture carbonate reservoir under different reservoir radius.

TABLE 3: Basic parameters of CT-2 in North Truva Oilfield.

Basic parameters	Value	Basic parameters	Value
Reservoir thickness/m	10.4	Compressibility factor/MPa <sup>-1</sup>	$3.3586 \times 10^{-3}$
Porosity/%	12.35	Density/g/cm <sup>3</sup>	0.6127
Viscosity/mPa·s	0.16	Initial reservoir pressure/MPa	32.731
Volume factor/dimensionless	1.952	Irreducible water saturation/%	33.09

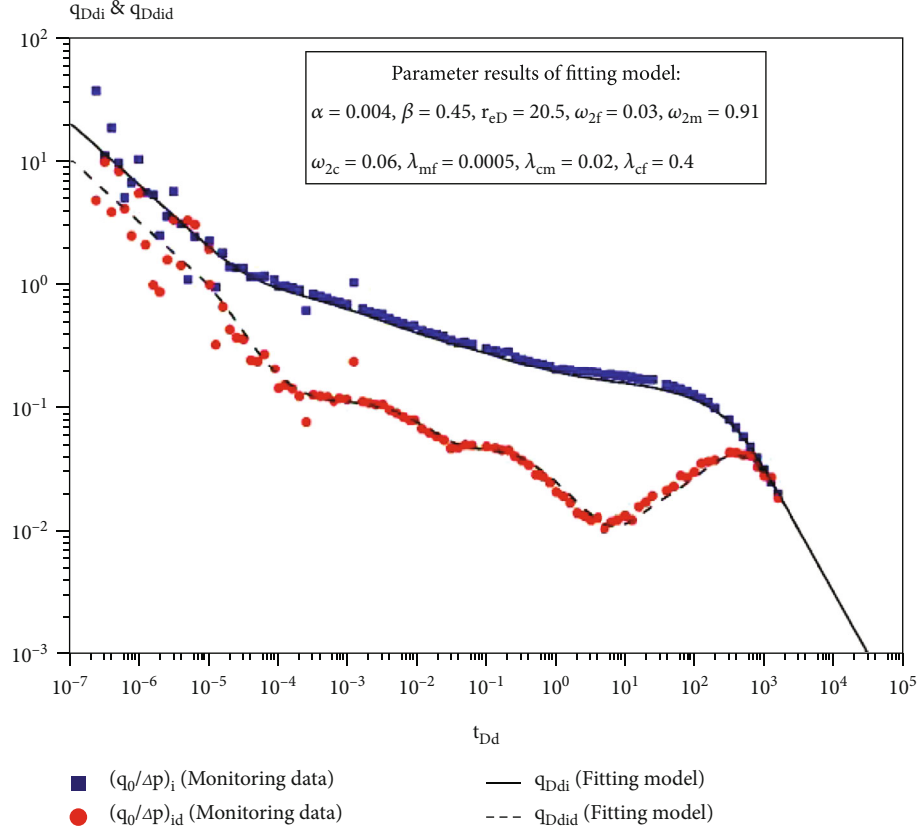


FIGURE 16: Fitting of monitoring data of CT-2 with new type rate decline curves.

TABLE 4: Fitting results of relevant parameters for CT-2.

Basic parameters	Value	Basic parameters	Value
Radius of stimulated area/m	18.5	Fracture elastic storability ratio/%	3
Reservoir radius/m	380	Matrix elastic storability ratio/%	91
Natural fracture permeability/ $10^{-3}\mu\text{m}^2$	27.7	Cavity elastic storability ratio/%	6
Skin factor/dimensionless	1.13	Matrix-fracture crossflow coefficient/dimensionless	0.0005
Interzonal diffusivity ratio/fraction	0.004	Matrix-cavity crossflow coefficient/dimensionless	0.02
Interzonal conductivity ratio/fraction	0.45	Cavity-fracture crossflow coefficient/dimensionless	0.4

is shorter, but the third V-segment exhibits the opposite trend (Figure 13(c)). Compared with the conventional rate decline curves (Figure 8), the characteristics of crossflow regimes of these new rate decline derivative curves are more obvious, which is helpful to inverse the elastic storability ratios of triple media reservoir in well test.

### 5.2.3. Crossflow Coefficients of Triple Media Reservoir.

Figures 14(a)–14(c) show the new rate decline curves of an

AFVW under different crossflow coefficients, respectively. As shown in Figure 14, these crossflow coefficients only have a weak impact on the rate integral but have a great impact on the rate integral derivative in the crossflow regimes. In particular, the depth and duration of the second and third V-segments fluctuate greatly, comparing with the conventional rate decline curves under the same conditions (Figure 9). Hence, this amplification effect of data difference is conducive to improve the accuracy of well-test inversion.

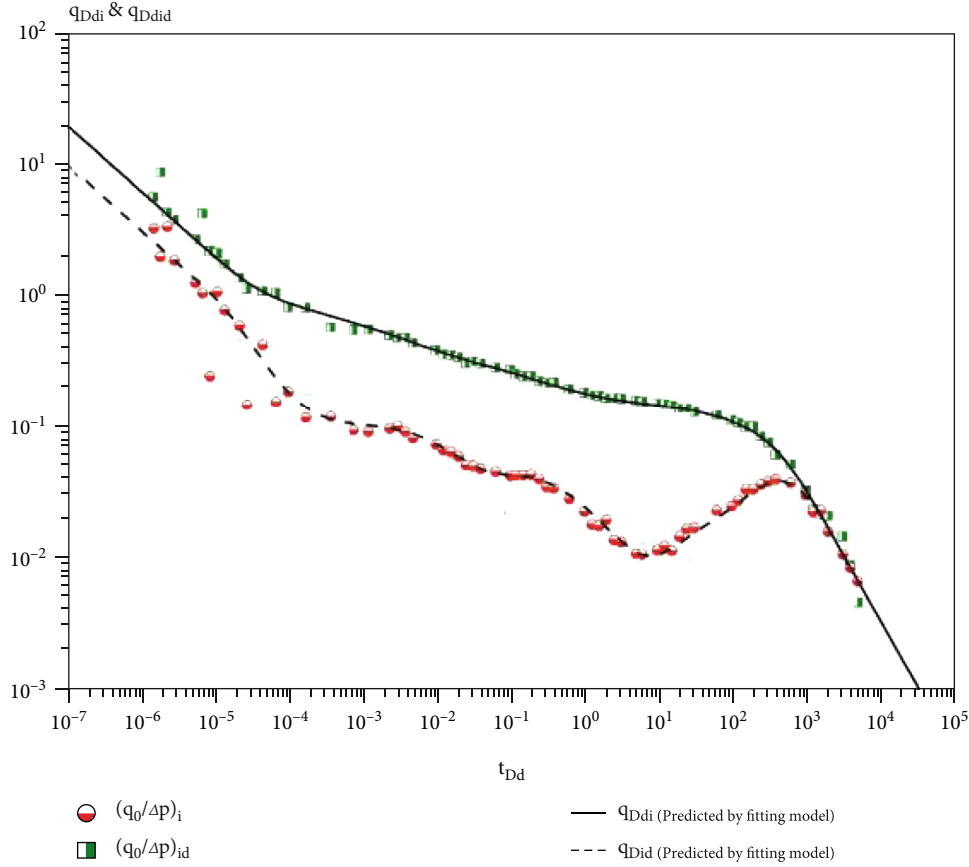


FIGURE 17: Comparison between predicted productivity and real productivity of CT-2.

5.2.4. *Compound Reservoir Radius.* Figure 15 presents the new rate decline curves of an AFVW under different reservoir radius. The main features are as follows: significant division appears in the early production period and the trend of rate integral derivative curves reverses four times; all the rate integral and rate integral derivative curves are completely normalized in the pseudo-steady flow regime. The occurrence time of the above characteristics is just opposite to the corresponding conventional rate decline curves (Figure 10).

In general, the new type rate decline curve has advantages over the conventional rate decline curve in the following aspects: (1) the characteristics of typical flow regimes are more significant and the occurrence of V-segments on the rate integral derivative curve improves the accuracy and efficiency of well-test inversion; (2) it can deal with the problem of variable flow rate and variable bottomhole pressure, facilitate on-site well test operation, reduce well shut-in time, and finally increase well productivity.

## 6. Field Application

CT-2 is an evaluation well located in North Truva oilfield in Kazakhstan. Nine-millimeter choke was used to control the blowout at the initial production stage and then acid fracturing was carried out to improve its well productivity. In order to analyze the reservoir seepage behavior and well productivity, a pressure gauge was put into the wellbore to monitor the dynamic change of bottomhole pressure before restart-

ing this well. Table 3 shows the basic parameters tested and calculated in the exploration and trial production stage.

Referring to the fitting procedures proposed by Pratikno et al. [31], the new rate decline curves calculated and drawn by our rate decline prediction model are used to fit the monitored bottomhole pressure and wellhead production data (Figure 16). Table 4 shows the fitting results of the relevant reservoir parameters, which is in line with the previous reservoir geological properties. Furthermore, these inversed parameters are used to predict the future productivity of CT-2, and the predicted productivity is basically consistent with its actual production performance after restarting this well (Figure 17), indicating that the newly developed rate decline prediction model for an AFVW in a pore-cavity-fracture carbonate reservoir has enough accuracy and meets the requirement of well test and production prediction.

## 7. Conclusions

This paper presents a new rate decline prediction model for an acid fracturing vertical well in a pore-cavity-fracture carbonate reservoir. Based on this work, several important conclusions are obtained:

- (1) The analytical solution and numerical solution of bottomhole pressure for an AFVW are basically consistent in the whole production period. Two kinds of solutions have their own advantages in well

test, the computing speed of numerical solution is faster, but the analytical solution is easier to deal with the problems such as wellbore storage, skin, and transient productivity

- (2) Acid fracturing has a weak effect on the instantaneous rate and cumulative productivity of an AFVW in the late period, but it significantly increases the early-period productivity, which is in line with the field requirement of rapid cost recovery and high production efficiency. A larger interzonal diffusivity ratio or a lower interzonal conductivity ratio is conducive to achieve higher early productivity. The reservoir properties like elastic storability ratio of natural fracture system, cavity-matrix crossflow coefficient, and reservoir radius strongly affect the instantaneous rate and cumulative productivity of an AFVW in the late stage
- (3) Using pseudo-steady constant derived by the progressive analysis method, a set of new rate decline curves are established, and six typical flow regimes can be observed. According to the reserve dominant types in triple media system, two or three V-segments occur on the rate integral derivative curves. Using the new rate decline curves for well test, the characteristics of flow regimes, like the depth and duration of V-segments, are remarkable and can improve well-test inversion accuracy, reduce shut-in time and then increase well productivity

## Nomenclature

### Field Variables

- $k$ : Permeability ( $10^{-3} \mu\text{m}^2$ )  
 $h$ : Formation thickness (m)  
 $\mu$ : Fluid viscosity (mPa·s)  
 $p$ : Pressure (MPa)  
 $r$ : Radial distance (m)  
 $r_f$ : Half-length of fractures and wormholes generated by acid fracturing (m)  
 $b$ : Width of fractures and wormholes generated by acid fracturing (m)  
 $t$ : Production time (d)  
 $\phi$ : Porosity, fraction  
 $c_i$ : Compressibility factor ( $\text{MPa}^{-1}$ )  
 $q$ : Total rate at the wellbore ( $\text{m}^3/\text{d}$ )  
 $B$ : Volume factor, dimensionless  
 $\gamma$ : Shape factor, dimensionless  
 $\eta$ : Fluid transmissivity factor, dimensionless  
 $N$ : Number of fractures and wormholes generated by acid fracturing, dimensionless.

### Dimensionless Variables: Real Domain

- $r_D$ : Dimensionless radius  
 $r_{eD}$ : Dimensionless reservoir radius  
 $r_{wD}$ : Dimensionless wellbore radius  
 $\Delta r_D$ : Dimensionless grid step of inner zone

- $\Delta r_{D1}$ : Dimensionless grid step of outer zone  
 $t_D$ : Dimensionless production time  
 $\Delta t_D$ : Dimensionless production time step  
 $p_D$ : Dimensionless pressure  
 $p_{1D}$ : Dimensionless pressure in inner zone  
 $p_{wD}$ : Dimensionless wellbore pressure  
 $p_{2fD}$ : Dimensionless pressure of natural fracture system in outer zone  
 $p_{2cD}$ : Dimensionless pressure of cavity system in outer zone  
 $p_{2mD}$ : Dimensionless pressure of matrix system in outer zone  
 $dp_D$ : Dimensionless pressure derivative  
 $q_{wD}$ : Dimensionless instantaneous rate  
 $q_{cD}$ : Dimensionless cumulative productivity  
 $p_{wD,ps}$ : Dimensionless wellbore pressure in pseudo-steady flow regime  
 $b_{Dps}$ : Dimensionless pseudo-steady constant  
 $t_{Dd}$ : Dimensionless decline time  
 $q_{Dd}$ : Dimensionless decline rate  
 $q_{Ddi}$ : Dimensionless rate integral  
 $q_{Ddid}$ : Dimensionless rate integral derivative.

### Dimensionless Variables: Laplace Domain

- $s$ : Time variable in Laplace domain  
 $x_1$ : Coefficient of general solution in Laplace domain  
 $x_2$ : Coefficient of general solution in Laplace domain  
 $\tilde{p}_{1D}$ : Dimensionless pressure in inner zone in Laplace domain  
 $\tilde{p}_{wD}$ : Dimensionless wellbore pressure in Laplace domain  
 $\tilde{p}_{2fD}$ : Dimensionless pressure of natural fracture in outer zone in Laplace domain  
 $\tilde{q}_{wD}$ : Dimensionless instantaneous rate in Laplace domain  
 $\tilde{q}_{cD}$ : Dimensionless cumulative productivity in Laplace domain.

### Greek Variables

- $\alpha$ : Interzonal diffusivity ratio  
 $\beta$ : Interzonal conductivity ratio  
 $\omega_{2f}$ : Elastic storability ratio of natural fracture system  
 $\omega_{2m}$ : Elastic storability ratio of matrix system  
 $\omega_{2c}$ : Elastic storability ratio of cavity system  
 $\lambda_{mf}$ : Matrix-fracture crossflow coefficient  
 $\lambda_{cf}$ : Cavity-fracture crossflow coefficient  
 $\lambda_{cm}$ : Cavity-matrix crossflow coefficient.

### Special Functions

- $I_0(x)$ : Modified Bessel function (1st kind, zero order)  
 $I_1(x)$ : Modified Bessel function (1st kind, first order)  
 $K_0(x)$ : Modified Bessel function (2nd kind, zero order)  
 $K_1(x)$ : Modified Bessel function (2nd kind, first order)  
 $\sinh(x)$ : Hyperbolic sine function  
 $\cosh(x)$ : Hyperbolic cosine function.

### Special Subscripts

- $w$ : Wellbore  
 $e$ : Reservoir external boundary



- 1: Inner zone  
 2f: Natural fracture system in outer zone  
 2c: Cavity system in outer zone  
 2m: Matrix system in outer zone  
 i: Initial condition or ordinal number  
 D: Dimensionless.

## Data Availability

The data used to support the findings of this study are included within the article.

## Conflicts of Interest

The authors declare that there are no conflicts of interest regarding the publication of this paper.

## Acknowledgments

The authors acknowledge that this study was funded by the National Natural Science Foundation of China (Program No. 52104031), the CNPC Innovation Foundation (Program No. 2020D-5007-0201), and the Natural Science Basic Research Program of Shaanxi (Program No. 2021JQ-596).

## References

- [1] W. Q. Li, L. X. Mu, L. Zhao et al., "Pore-throat structure characteristics and its impact on the porosity and permeability relationship of Carboniferous carbonate reservoirs in eastern edge of Pre-Caspian Basin," *Petroleum Exploration and Development*, vol. 47, no. 5, pp. 1027–1041, 2020.
- [2] J. X. Gao, C. B. Tian, W. M. Zhang, X. M. Song, and B. Liu, "Characteristics and genesis of carbonate reservoir of the Mishrif Formation in the Rumaila oil field, Iraq," *Acta Petrolei Sinica*, vol. 34, no. 5, pp. 843–852, 2013.
- [3] D. Q. Zhang, S. Q. Wang, W. Q. Zhao, Z. F. Fan, and Z. P. Li, "The main geological control factors of single well productivity for carbonate reservoir: take the reservoir formation KT-I in North Truva field, Kazakhstan as example," *Acta Petrologica Sinica*, vol. 32, no. 3, pp. 903–914, 2016.
- [4] X. L. Zhang, Y. L. Hu, R. Fan, Y. W. Jiao, and S. L. Zhang, "Research on the developing strategies of the fracture-cavern carbonate oil reservoir in Tarim oilfield," *Journal of Southwest Petroleum University (Science & Technology Edition)*, vol. 32, no. 6, pp. 107–112, 2010.
- [5] J. E. Warren and P. J. Root, "The behavior of naturally fractured reservoirs," *Society of Petroleum Engineers Journal*, vol. 3, no. 3, pp. 245–255, 1963.
- [6] J. Liu, G. S. Bodvarsson, and Y. S. Wu, "Analysis of flow behavior in fractured lithophysal reservoirs," *Journal of Contaminant Hydrology*, vol. 62–63, pp. 189–211, 2003.
- [7] Y. S. Wu, G. Qin, R. E. Ewing, Y. Efendiev, Z. J. Kang, and Y. L. Ren, "A multiple-continuum approach for modeling multiphase flow in naturally fractured vuggy petroleum reservoirs," in *International Oil & Gas Conference and Exhibition*, Beijing, China, 2006.
- [8] Y. S. Wu, C. A. Ehlig-Economides, G. Qin et al., "A triple-continuum pressure-transient model for a naturally fractured vuggy reservoir," in *SPE Annual Technical Conference and Exhibition*, Anaheim, California, America, 2007.
- [9] Q. Zhang, *Principle and Design of Oil Production Engineering*, China University of Petroleum Press, Dongying, Shandong, China, 2006.
- [10] M. Liu, S. C. Zhang, and J. Y. Mou, "Fractal nature of acid-etched wormholes and the influence of acid type on wormholes," *Petroleum Exploration and Development*, vol. 39, no. 5, pp. 630–635, 2012.
- [11] H. J. Chen, J. C. Guo, and J. Z. Zhao, "Laboratory damage appraisal and cleaning technology of hydraulic fractures," *Petroleum Exploration and Development*, vol. 31, no. 4, pp. 136–138, 2004.
- [12] S. C. Zhang, Z. F. Zhuang, J. Li, X. Zhao, and Q. Wang, "Effects of natural gas on viscoelastic surfactant (VES) fracturing fluids," *Natural Gas Industry*, vol. 28, no. 11, pp. 85–87, 2008.
- [13] M. Economides, R. Oligney, and P. Valko, *Unified Fracture Design: Bridging the Gap between Theory and Practice*, Orsa Press, Alvin, Texas, America, 2002.
- [14] M. Prats, "Effect of vertical fractures on reservoir behavior-incompressible fluid case," *Society of Petroleum Engineers Journal*, vol. 1, no. 2, pp. 105–118, 1961.
- [15] A. C. Gringarten, H. J. Ramey Jr., and R. Raghavan, "Unsteady-state pressure distributions created by a well with a single infinite-conductivity vertical fracture," *Society of Petroleum Engineers Journal*, vol. 14, no. 4, pp. 347–360, 1974.
- [16] H. Cinco-Ley and F. Samaniego-V, "Transient pressure analysis for fractured wells," *Journal of Petroleum Technology*, vol. 33, no. 9, pp. 1749–1766, 1981.
- [17] L. Xiao and G. Zhao, "Study of 2-D and 3-D hydraulic fractures with non-uniform conductivity and geometry using source and sink function methods," in *SPE Canadian Unconventional Resources Conference*, Calgary, Alberta, Canada, 2012.
- [18] Z. M. Chen, X. W. Liao, X. L. Zhao, X. J. Dou, and L. T. Zhu, "Performance of horizontal wells with fracture networks in shale gas formation," *Journal of Petroleum Science and Engineering*, vol. 133, pp. 646–664, 2015.
- [19] W. J. Luo, X. D. Wang, C. F. Tang, Y. Feng, and E. X. Shi, "Productivity of multiple fractures in a closed rectangular reservoir," *Journal of Petroleum Science and Engineering*, vol. 157, pp. 232–247, 2017.
- [20] Z. W. Wu, C. Z. Cui, G. Z. Lv, S. X. Bing, and G. Cao, "A multi-linear transient pressure model for multistage fractured horizontal well in tight oil reservoirs with considering threshold pressure gradient and stress sensitivity," *Journal of Petroleum Science and Engineering*, vol. 172, pp. 839–854, 2019.
- [21] D. P. Restrepo, *Pressure Behavior of a System Containing Multiple Vertical Fractures*, University of Oklahoma, Norman, Oklahoma, America, 2008, Doctoral Dissertation.
- [22] L. Wang, X. D. Wang, E. H. Luo, and J. H. Wang, "Analytical modeling of flow behavior for wormholes in naturally fractured-vuggy porous media," *Transport in Porous Media*, vol. 105, no. 3, pp. 539–558, 2014.
- [23] Z. M. Chen, X. W. Liao, C. H. Huang et al., "Productivity estimations for vertically fractured wells with asymmetrical multiple fractures," *Applications in Engineering Science*, vol. 21, pp. 1048–1060, 2014.
- [24] D. Chuprakov, I. Bekerov, and A. Iuldasheva, "Productivity of hydraulic fractures with heterogeneous proppant placement and acid etched walls," *Applications in Engineering Science*, vol. 3, pp. 100018–100023, 2020.

- [25] C. P. Chiang and W. A. Kennedy, "Numerical simulation of pressure behavior in a fractured reservoir," in *in Fall Meeting of the Society of Petroleum Engineers of AIIME*, Houston, Texas, America, 1970.
- [26] J. Douglas and D. W. Peaceman, "Numerical solution of two-dimensional heat-flow problems," *AICHE Journal*, vol. 1, no. 4, pp. 505–512, 1955.
- [27] E. Ozkan, *Performance of Horizontal Wells*, Tulsa University, Tulsa, Oklahoma, America, 1988, Doctoral Dissertation.
- [28] A. F. Van Everdingen and W. Hurst, "The application of the Laplace transformation to flow problems in reservoirs," *Journal of Petroleum Technology*, vol. 1, no. 12, pp. 305–324, 1949.
- [29] M. J. Fetkovich, "Decline curve analysis using type curves," *Journal of Petroleum Technology*, vol. 32, no. 6, pp. 1065–1077, 1980.
- [30] T. A. Blasingame, T. L. McCray, and W. J. Lee, "Decline curve analysis for variable pressure drop/variable flowrate systems," in *in SPE Gas Technology Symposium*, Houston, Texas, America, 1991.
- [31] H. Pratikno, J. A. Rushing, and T. A. Blasingame, "Decline curve analysis using type curves - fractured wells," in *in SPE Annual Technical Conference and Exhibition*, Denver, Colorado, America, 2003.